Detection of extracellular enteropathogens by intracellular sensors

A Thesis

submitted to

Indian Institute of Science Education and Research Pune in partial fulfilment of the requirements for the BS-MS Dual Degree Programme

by

Ishaan Chaudhary

Indian Institute of Science Education and Research Pune

Dr. Homi Bhabha Road,

Pashan, Pune 411008, INDIA.

Date: March, 2026

Under the guidance of

Supervisor: Dr. Avinash Shenoy

Reader in Innate Immunology and Infection, Department of Infectious Diseases, Imperial College, London

From May 2025 to Mar 2026

INDIAN INSTITUTE OF SCIENCE EDUCATION AND RESEARCH PUNE

Certificate

This is to certify that this dissertation entitled **Detection of extracellular enteropathogens by intracellular sensors** towards the partial fulfilment of the BS-MS dual degree programme at the Indian Institute of Science Education and Research, Pune represents study/work carried out by Ishaan Chaudhary at Imperial College, London, under the supervision of Dr. Avinash Shenoy, Reader in Innate Immunology and Infection, Department of Infectious Diseases during the academic year 2025-2026.

Dr. Avinash Shenoy

Committee:

Dr. Avinash Shenoy

Dr. Nishad Matange

This thesis is dedicated to my friends and family, and to the honest and curious spirit with which we do science.

Declaration

I hereby declare that the matter embodied in the report entitled "**Detection of extracellular enteropathogens by intracellular sensors**" are the results of the work carried out by me at the Department of Infectious Diseases , Imperial College London, under the supervision of Dr. Avinash Shenoy, and the same has not been submitted elsewhere for any other degree. Wherever others contribute, every effort is made to indicate this clearly, with due reference to the literature and acknowledgement of collaborative research and discussions. Part of the work done in this thesis has been submitted for a manuscript which is currently under revision (Bennison *et al.*, 2025).

Ishaan Chaudhary

20211050

Table of Contents

List of Tables

List of Figures

Abstract

Enteropathogenic *E. coli* (EPEC) and Enterohaemmorhagic *E. coli* (EHEC) are extracellular Gram-negative enteric pathogens that cause diarrhoeal disease in humans. They cause actin polymerisation downstream of intimin-induced clustering of Type-3 Secretion System effector Tir (Translocated intimin receptor), leading to the formation of pedestals. Guanylate Binding Protein 1 (GBP1) and caspase-4 are cytosolic lipopolysaccharide (LPS) sensors involved in detecting and responding to cytosolic Gram-negative pathogen infections. However, the role of GBP1 and caspase-4 in epithelial cells upon extracellular pathogen infection remains unknown. In this study, we investigate the mechanisms involved in detecting EPEC and EHEC infections in intestinal epithelial cells by the intracellular sensors GBP1 and caspase-4. We show that epithelial cells recognise extracellular pathogen infection in a GBP1 and caspase-4-dependent manner. This mechanism is gasdermin-D-dependent and NLRP3-caspase-1-independent. We observe recruitment of caspase-4 to actin pedestals at sites of infection in a GBP1-dependent manner and determine that GBP1 is essential in intestinal epithelial cells for full pyroptotic response to extracellular enteropathogens. We demonstrate that the recruitment of cytosolic sensors GBP1 and caspase-4 to sites of extracellular pathogen infections in epithelial cells is LPS-independent and requires only actin polymerisation triggered by Tir-clustering at the cell membrane. Our study broadens the scope of GBP1 as a cytosolic immune sensor and provides evidence for its role in LPS-independent pathogen sensing mechanisms. The observation that GBP1 is involved in the detection of extracellular pathogens is of consequence to future studies that may investigate the involvement of cytosolic sensors in immune responses to other pathogens.

Acknowledgements

I would like to thank Dr. Avinash Shenoy for his constant support and guidance without which this project would not have been possible. I am extremely grateful for his constant presence and help at a moment's notice, and for ensuring the continuous availability of lab equipment and materials for smooth execution of the project. I would also like to thank present and past members of the Shenoy lab, Ayush Punwatkar, Justin Wong, Ella Rellis, Dharitri Chaudhuri, Miyu Stephenson, Zoha Sohail, and Chinmay Patwardhan, who guided me and made daily life friendly and pleasant.

I am forever thankful to my family who ensured I was alright in a foreign country, and to all my friends, especially Aparajita, Deep, Apoorvaa, Deepika, Sidharth, Ameya, Pranav, Kartik, Paritosh, Harsh, Kishan, Seona, Sahil, Jai, Gayathri, Abhinav, Yash, Chinmayee, Ayushi and Aditya, for all their love and support.

I would specially like to thank my dearest friend, Gaadha Vinukumar, who was always rooting for me, and was with me through all the ups and downs of this journey and never let me feel alone.

Finally, I would like to thank the Indian Institute of Science Education and Research, Pune for giving me this wonderful opportunity to conduct my Masters Thesis and Imperial College London, for providing me with a suitable environment, campus and facilities to conduct my research. I extend my gratitude to all the people working behind the scenes, the administrative, management and housekeeping staff who ensured proper functioning of institutions and facilities.

Contributions

Contributor name	Contributor role
Avinash Shenoy, Daniel Bennison	Conceptualisation Ideas
Ishaan Chaudhary, Avinash Shenoy,	Methodology
Ishaan Chaudhary, Avinash Shenoy	Software
Ishaan Chaudhary	Validation
Ishaan Chaudhary	Formal analysis
Ishaan Chaudhary, Daniel Bennison, Avinash Shenoy, Ayush Punwatkar, Miyu Stephenson	Investigation
Avinash Shenoy	Resources
Ishaan Chaudhary	Data Curation
Ishaan Chaudhary	Writing - original draft preparation
Ishaan Chaudhary, Avinash Shenoy	Writing - review and editing
Ishaan Chaudhary, Avinash Shenoy, Daniel Bennison	Visualisation
Avinash Shenoy	Supervision
Avinash Shenoy	Project administration
Avinash Shenoy	Funding acquisition

I declare that no Generative AI was used in this thesis.

1. Introduction

1.1. Diarrhoeagenic enteric bacterial pathogens

Diarrhoeagenic diseases affect a large proportion of people in the world, leading to nearly 1200 deaths just among young children everyday (Chaudhuri *et al.*, 2026; Diarrhoea UNICEF). These diseases may be caused by invasive pathogens such as *Salmonella* and *Shigella* leading to diseases such as typhoid and shigellosis or extracellular pathogens such as Diarrhoeagenic *E. coli* (DEC) (Cabrera-Sosa and Ochoa, 2020; Zong Minko *et al.*, 2024). Diarrhoeal diseases are the third largest cause of death in children aged 1-5 (Diarrhoeal disease WHO). DEC are responsible for 30 - 40% of all diarrhoeal cases in children in Low and Middle-Income Countries (LMIC). DEC-induced diseases present in many forms such as haemolytic uraemic syndrome (HUS) and infantile diarrhoea (Cabrera-Sosa and Ochoa, 2020). If improperly diagnosed or left untreated, these diseases can prove to be fatal.

The DEC pathotype Enteropathogenic *E. coli* (EPEC) is the leading cause of infantile diarrhoea, i.e., death in children below the age of 5 with a disproportionally high load in LMICs (Cabrera-Sosa and Ochoa, 2020; Chaudhuri *et al.*, 2026). Although usually mild, it can present with fever and vomiting, and if left untreated can lead to malnutrition and ultimately death (Kotloff *et al.*, 2013; Cabrera-Sosa and Ochoa, 2020). Enterohaemmorhagic E. coli (EHEC) is a type of Shiga toxin-producing *E. coli* (STEC) and is the primary causative agent of HUS (Sperandio and Pacheco, 2012). STEC causes diarrhoea in all age groups and is a major cause of concern in high-income countries; estimates suggest nearly 3 million acute STEC-related illnesses annually worldwide (Majowicz *et al.*, 2014). STEC infections often present with bloody diarrhoea and abdominal cramps, and in severe cases they lead to HUS, characterised by acute renal failure, thrombocytopenia, and microangiopathic haemolytic anaemia (Sperandio and Nguyen, 2012; Smith *et al.*, 2014).

The molecular mechanisms leading to diarrhoea involve the inhibition of sodium glucose cotransporter-1 (SGLT1), DRA (a Cl^-/OH^- exchanger) and NHE3 (a Na^+/H^+ exchanger, also called SLC9A3), leading to an accumulation of sodium and chloride ions in the lumen of the intestine, creating an osmotic imbalance and leaching water

by exosmosis out of cells into the lumen, leading to dehydration and runny stool (Dean and Kenny, 2009).

EPEC and EHEC can cause diarrhoea by attaching extracellularly and injecting pathogenic effectors into the host cytoplasm which can upset this osmotic balance (Kenny and Finlay, 1997; Frankel *et al.*, 1998). Some of these effectors also suppress immune response against these pathogens (Pallett *et al.*, 2017; Luchetti *et al.*, 2025). However, cytokines can “prime” the innate immune system to sense and respond to these infections (Tretina *et al.*, 2019), but the molecular mechanisms involved in sensing EPEC and EHEC require further elucidation.

A

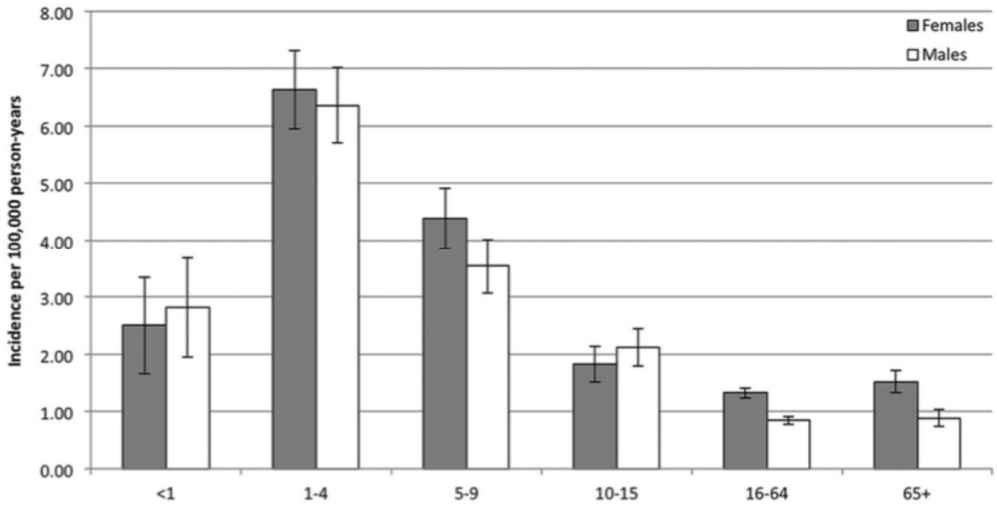

B

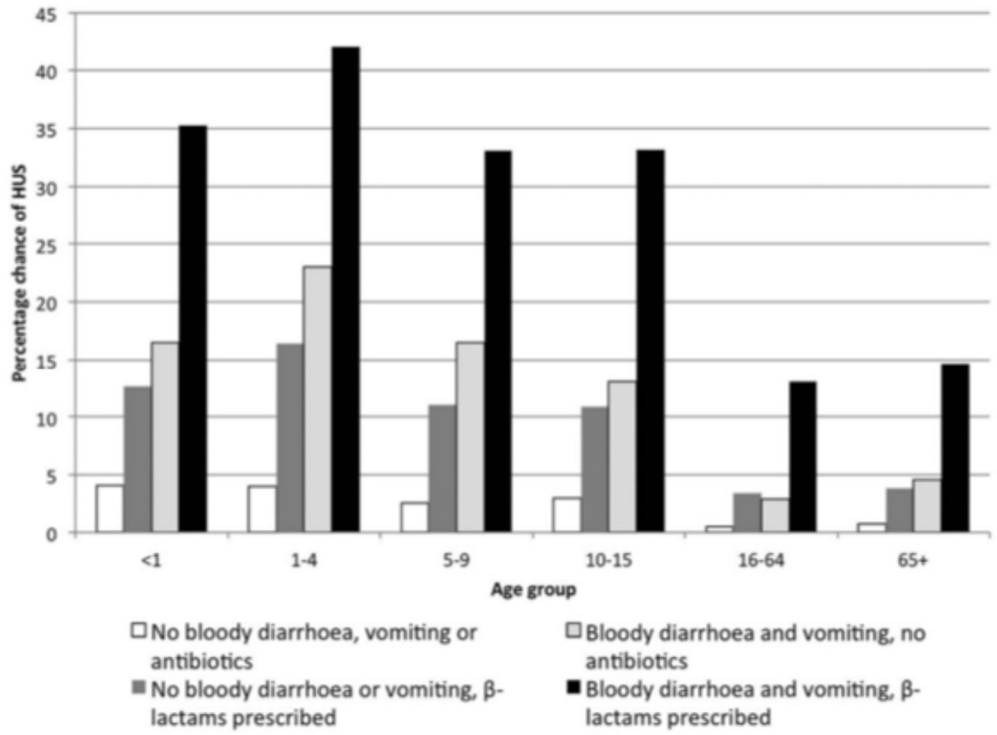

Figure 1 taken from (Launders *et al.*, 2016). Bar charts depicting incidence of STEC infections and percentage of STEC infections leading to HUS.

(A) Bar chart depicting incidence of symptomatic STEC O157 infections from 2009-2012 sorted by age groups and gender.

(B) Bar chart depicting predictive percentage chance of STEC O157 infection cases developing Haemolytic Uraemic Syndrome (HUS)

1.2. Attaching/Effacing Pathogens

Attaching/Effacing (A/E) pathogens refer to bacterial pathogens that attach extracellularly to intestinal cell membranes and efface their brush border microvilli, leading to the formation of “attaching/effacing” (A/E) lesions at sites of infection (Frankel *et al.*, 1998). Two A/E pathogens which infect human intestinal epithelia are EPEC and EHEC. They reside extracellularly and inject various pathogenic effectors into the cell through the assembly of a Type-3 Secretion System (T3SS) injectosome, which acts as a microscopic injection needle, piercing through the host cell membrane and allowing the secretion of bacterial proteins into the host cytosol (Shenoy *et al.*, 2018). Many such effectors are located on the *Locus of Enterocyte Effacement* (LEE) pathogenicity island, one of which is the Translocated Intimin Receptor (Tir) (McDaniel *et al.*, 1995; Elliott *et al.*, 1998). Tir is translocated into the host cell membrane, and forms a hairpin structure, with an intimin-binding region exposed into the extracellular matrix. Here, Tir interacts with its ligand intimin on the bacterial outer membrane to form intimate attachments, allowing the bacteria to reside extracellularly (Wong *et al.*, 2011; Pearson *et al.*, 2016). This leads to effacement of the brush border epithelia present on the apical enterocyte membrane, forming A/E lesions, characteristic of EPEC and EHEC infections (Knutton *et al.*, 1987). Some strains of EPEC, termed typical EPEC, also contain the *E. coli* adherence factor (EAF) plasmid, which encodes the bundle-forming pilus (BFP), allowing EPEC to form microcolonies at sites of infection on enterocytes (Donnenberg *et al.*, 1992).

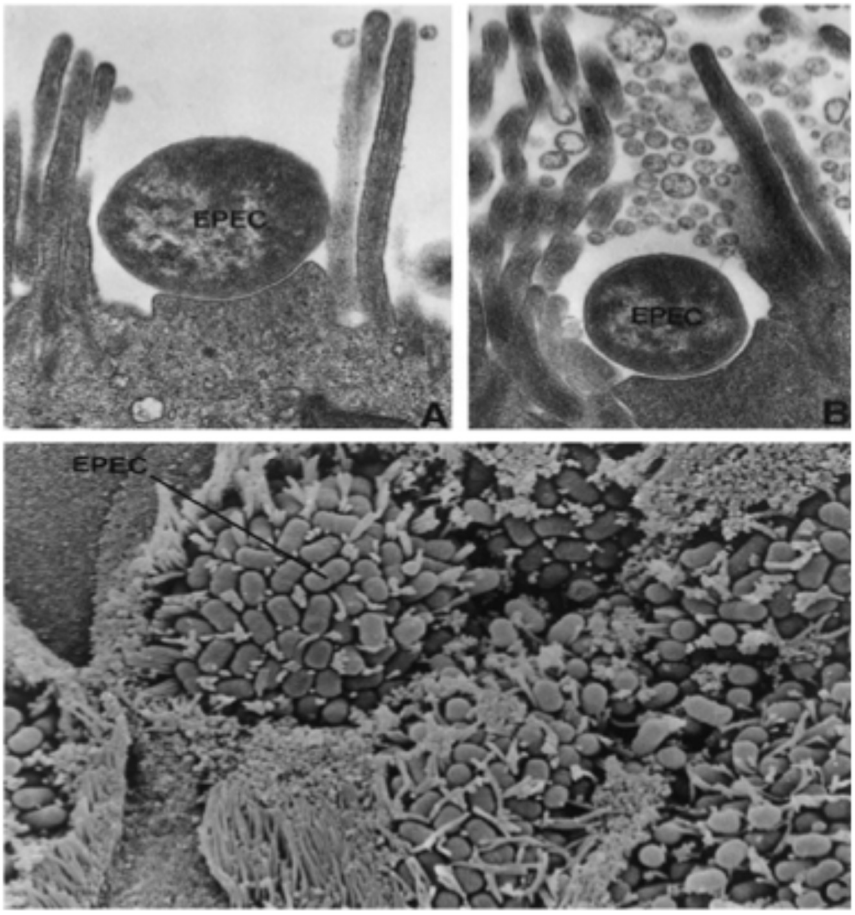

Figure 2 taken from (Knutton *et al.*, 1987) and (Frankel *et al.*, 1998). Electron micrographs depicting EPEC pedestal formation and microvilli effacement.

(A) Electron micrograph showing intimate bacterial attachment and pedestal formation.

(B) Electron micrograph illustrating brush-border effacement through microvilli destruction.

(C) Localised microvilli brush border architecture destruction upon EPEC infection.

Intimin-mediated Tir clustering at sites of infection initiates signalling for the formation of actin pedestals (Wong *et al.*, 2011; Pearson *et al.*, 2016). Downstream of Tir clustering, EPEC and EHEC differ slightly in their mechanisms of pedestal formation. Tir^{EPEC} is phosphorylated by host Src kinases (at Y474), which leads to recruitment of adapter proteins Nck1/2 (non-catalytic region of tyrosine kinase adaptor protein 1/2). Further, NWASP (Neuronal Wilkott-Aldrich Syndrome Protein) is recruited (Kenny *et al.*, 1997; Phillips *et al.*, 2004), along with ARP2/3 to initiate actin polymerisation (Gruenheid *et al.*, 2001). In contrast, EHEC recruits NWASP via another effector, TccP (Tir cytoskeleton coupling protein, also called *E. coli* secreted protein F-like from prophage U, $EspF_U$). TccP is recruited to Tir via one of two host proteins, IRTKS

(Insulin receptor tyrosine kinase substrate) or IRSp53 (Insulin Receptor Substrate p53) (Vingadassalom *et al.*, 2009; Weiss *et al.*, 2009; Crepin *et al.*, 2010). Through these mechanisms, EPEC and EHEC form characteristic “actin pedestals” underneath sites of infections (Frankel and Phillips, 2008). These actin pedestals may play a role in sensing these infections; however, their exact function remains unclear.

EPEC and EHEC also use many effectors to cause disease, manipulate host immune signalling and evade immune defence systems. Two effectors involved in manipulating host immune responses are the non-LEE-encoded effectors *nleL* and *nleF*. NleL is a HECT-like E3 ubiquitin ligase that targets proteins such as caspase-4, ROCK1 and ROCK2 for proteasomal degradation (Luchetti *et al.*, 2025). NleF has been reported to bind to the catalytic domain of caspase-4 and inhibit its proteolytic activity (Pallett *et al.*, 2017). Other LEE and non-LEE effectors are also important for successful colonisation of A/E pathogens. *Citrobacter rodentium* is a mouse infection model used to model A/E infections in vivo (Deng *et al.*, 2003; Collins *et al.*, 2014; Mullineaux-Sanders *et al.*, 2019), and knocking out Tir (Schauer and Falkow, 1993), intimin (Deng *et al.*, 2003), or a functional T3SS system (Petty *et al.*, 2010) in *C. rodentium* renders it completely avirulent. Deleting *nleA* (Gruenheid *et al.*, 2004) or *nleB* (Kelly *et al.*, 2006) also leads to highly attenuated virulence in *C. rodentium*, indicating an important role for these effectors in effective colonisation of the murine gut. Diarrhoeal disease is caused by disruption of tight junctions in intestinal epithelia leading to “leaky junctions” by effectors such as Map (Mitochondria-associated protein), EPEC-secreted proteins EspF, EspG, and NleA (Ma *et al.*, 2006).

Innate immune proteins in these epithelia act as a first line of defence against pathogens by detecting and mounting an effective immune response to them (Fisch *et al.*, 2019). However, the molecular mechanisms by which the innate immune system responds to A/E pathogen infection is not well characterised.

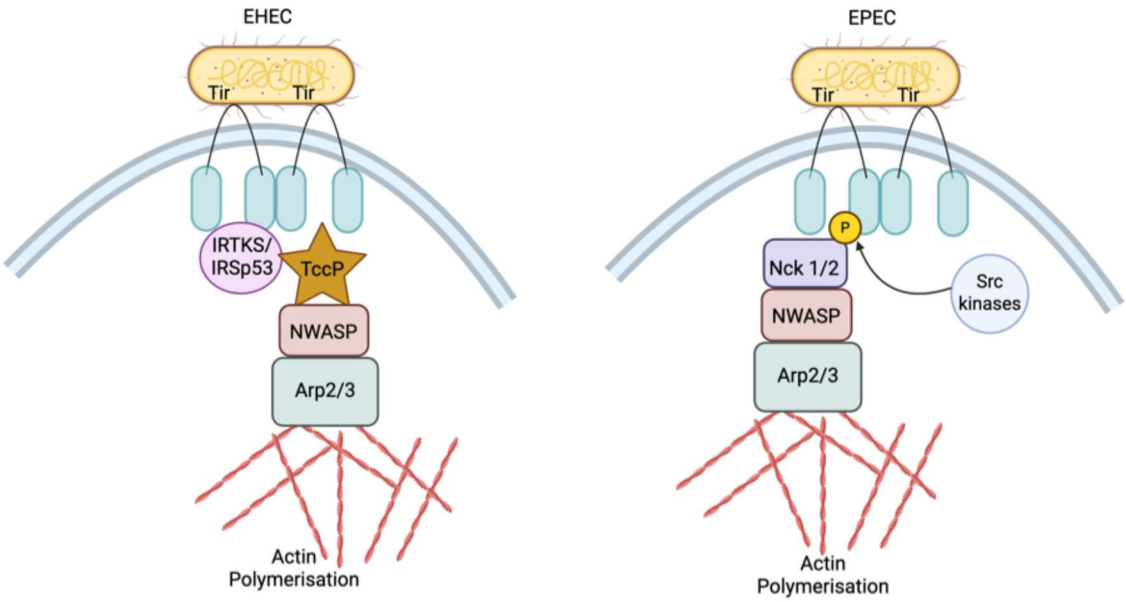

Figure 3: Schematic depicting major differences between EPEC and EHEC-induced mechanisms of actin polymerisation. Created in BioRender.

Figure shows actin polymerisation downstream of Intimin-mediated Tir clustering upon EPEC and EHEC infections. EPEC infections involve Nck 1/2 recruitment to phosphorylated Tir, whereas EHEC involves IRSp53 or IRTKS-mediated recruitment of bacterial TccP/EspF$_U$.

1.3. The innate immune system

Cell-autonomous immune sensing acts as a first line of defence against invading pathogens. The innate immune system can recognise infections by recognising common Pathogen Associated Molecular Patters (PAMPs) through PAMP-triggered immunity, or common pathogenic effectors through effector-triggered immunity (Janeway, 1989; Stuart *et al.*, 2013). PAMPs are recognised by Pattern Recognition Receptors (PRRs). PRRs may be present as receptors on the cell membrane such as Toll-Like Receptors (TLRs) to recognise extracellular threats or may be present in the cytosol such as inflammasomes to recognise invasive pathogens in the cytosol or in vacuoles. TLR4 can recognise bacterial membrane components such as lipopolysaccharide (LPS) (Varma *et al.*, 2005; Murphey *et al.*, 2007)and monophosphoryl Lipid A (MPLA) (Romero *et al.*, 2011; Fensterheim *et al.*, 2018), whereas TLR2 can recognise peptidoglycan (Murphey and Sherwood, 2008).

Inflammasomes are cytosolic multi-protein immune sensing complexes which detect and respond to incoming dangers (Broz and Dixit, 2016). NLRP3 (NOD, leucine-rich repeat and Pyrin domain-containing protein 3) is an inflammasome complex which senses danger by sensing K^+ efflux out of the cell (Broz *et al.*, 2010; Man *et al.*, 2014; Fisch *et al.*, 2019). Two distinct mechanisms can lead to this K^+ efflux, the canonical and non-canonical inflammasome activation pathways.

Canonical inflammasome activation is triggered by the opening of P2X7 channels by ligands such as ATP or bacterial toxins such as nigericin (Broz and Dixit, 2016). Non-canonical inflammasome activation involves cytosolic LPS detection by caspase-4, leading to activation of its protease activity. Caspase-4 then cleaves the molecule gasdermin-D (GSDMD). The N-terminal fragment of GSDMD oligomerises at the plasma membrane, forming large pores, leading to K^+ efflux and eventually to cell death through an inflammatory mode of cell death known as pyroptosis (Sanchez-Garrido *et al.*, 2020). The non-canonical inflammasome pathway plays a crucial role in the defence against cytosolic Gram-negative pathogens such as *Salmonella*, *Shigella* and *Burkholderia* (Ceballos-Olvera *et al.*, 2011; Fisch *et al.*, 2019; Li *et al.*, 2020). Upon activation, NLRP3, through the ASC (apoptosis-associated speck-like protein containing a CARD) adapter protein, cleaves caspase-1, which further cleaves the pro-inflammatory cytokines IL-1β and IL-18 (Sanchez-Garrido *et al.*, 2020). Inflammasome-mediated pyroptosis and cytokine release act as important cues to eliminate pathogen replicative niches and warn nearby cells of impending danger.

In THP-1 macrophages, the NLRP3-caspase-1 inflammasome plays an important role in the detection and pyroptotic response to EPEC infections, downstream of caspase-4 (Fisch *et al.*, 2019). Although caspase-4 is also involved in detection of cytosolic infections in epithelial cell lines, the role of NLRP-3-caspase-1 or caspase-4 has not yet been studied in epithelial cell response to extracellular pathogens such as EPEC and EHEC. However, epithelial cells do not pyroptose upon enteropathogenic infections without cytokine priming (data not shown), thus it is imperative to study the role of cytokines in priming and activating caspases, and in inflammasome pathways in immune responses of epithelial cells to these pathogens.

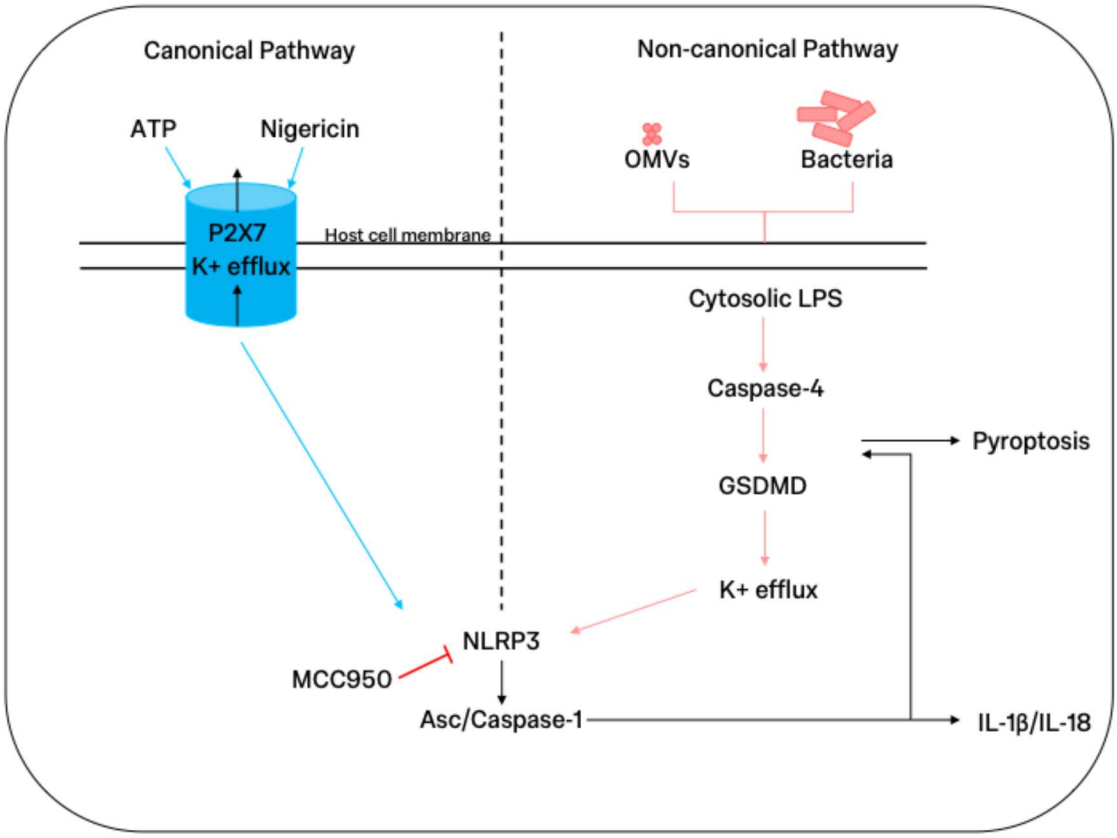

Figure 4: Schematic depicting canonical and non-canonical modes of NLRP3 inflammasome activation.

The canonical mode of activation involves K^+ efflux through P2X7 ion channels triggered by ligands such as ATP and bacterial nigericin. The non-canonical inflammasome pathway is triggered by LPS from bacteria or outer membrane vesicles (OMVs) making their way into the cytoplasm, leading to recognition by caspase-4, which further cleaves GSDMD and causes K^+ efflux. MCC950 is a potent NLRP3 inhibitor.

1.4. Cytokines – Interleukins and Interferons

Cytokines such as interleukins and interferons are critical drivers of immune responses to infections. Pro-inflammatory cytokines such as interleukin 1β (IL-1β), IL-18 and interferon-γ (IFNγ) are secreted cytokines which play an important role in priming cellular defence against infection by stimulating immune cell recruitment and activation, increasing vascular permeability and inducing fever (Al-Qahtani *et al.*, 2024).

IL-1β and IL-18 belong to the IL-1 family of interleukins. These cytokines bind to the IL-1 receptor and initiate signalling pathways to produce other inflammatory

molecules and recruit immune cells to sites of infection (Veerdonk *et al.*, 2011). Both the cytokines are present in their inactive pro-forms in the cytoplasm and need proteolytic cleavage, primarily through caspase-1 to activate and get released into the extracellular matrix (Veerdonk *et al.*, 2011; Sanchez-Garrido *et al.*, 2020). IL-1β plays a role in activating the adaptive immune system and improves mucosal host defence. It initiates T helper cell response which improves mucosal barrier function during infection by secreting IL-17 and IL-22 that stimulate the release of antimicrobial peptides and chemokines for neutrophil recruitment (Al-Qahtani *et al.*, 2024). IL-18 binds to the IL-18 receptor and activates and upregulates the cytotoxic function of CD-8 T-cells and Natural Killer (NK) cells. It also initiates a signalling cascade leading to the production of other cytokines such as IL-4, IL-13, Tumour Necrosis Factor(TNF) and Interferon-γ (IFNγ) (Ihim *et al.*, 2022).

IFNγ is a Type II interferon that confers many protective functions during infection. In macrophages, IFNγ can enhance antigen presentation by upregulating Class-II MHC molecules, it can increase reactive oxygen and nitrogen species production and induce autophagy to clear intracellular pathogens. IFNγ also upregulates the production of various anti-microbial molecules to detect and defend against infections (Ng *et al.*, 2023). In the context of bacterial infections in intestinal epithelial cells, IFNγ is crucial for successful pyroptotic response (Bennison *et al.*, 2025). Without IFNγ-priming, intestinal epithelia are unable to effectively respond to bacterial infections. One important group of interferon-stimulated genes (ISGs) involved in pyroptotic response is the group of GTPases termed the Guanylate Binding Proteins (GBPs) (Bennison *et al.*, 2025).

1.5. Guanylate Binding Proteins – Interferon-induced GTPases

Guanylate Binding Proteins (GBPs) are Interferon-γ-induced dynamin-like large GTPases that play a crucial role in antimicrobial defence (Kim *et al.*, 2011; Shenoy *et al.*, 2012; Tretina *et al.*, 2019). GBPs are involved in the defence against various bacterial pathogens such as *Salmonella enterica, Shigella flexneri, Francisella novicida, Yersinia enterocolitica* and *Chlamydia trachomatis* to name a few. They have also been implicated in immune roles in the detection and response to protozoan pathogens such as *Toxoplasma gondii* and *Leishmania donovani* (Fisch *et*

al., 2019; Rivera-Cuevas *et al.*, 2023). GBP1 is the most well-studied of seven human GBP family members, and past work from the Shenoy lab has investigated the role of GBP1 against intracellular pathogens such as *Salmonella* and *Toxoplasma*. They showed that GBP1 coats the surface of cytosolic *Salmonella*. They also showed that GBP1 is recruited to *Toxoplasma*-containing vacuoles, and targets them for rupture, uncovering broader roles for GBP1 in anti-microbial defence beyond Gram-negative bacteria (Fisch *et al.*, 2019).

GBPs contain a C-teminal CaaX isoprenylation motif which is post-translationally modified to facilitate recruitment to membranes. GBP1, GBP2 and GBP5 contain a CaaX motif which is modified with either a 15-carbon farnesyl group (GBP1) or a 20-carbon geranylgeranyl group (GBP2 and GBP5) (Nantais *et al.*, 1996; Britzen-Laurent *et al.*, 2010). Past reports have shown that these post-translational modifications are crucial for the antimicrobial function of GBPs, indicating that physical engagement with membranes plays an important role in the conformational changes which activate GBP function in innate immunity.

Crystal structures of GBP1, and recently, cryo-electron microscopy structures of GBP1 have provided further clues about the mechanism by which GBP1 performs its antimicrobial activity. It dimerises via a highly conserved “G-interface”, leading to its GTPase activity stimulation (Kuhm *et al.*, 2025). GBP1 catalyses GTP hydrolysis in two distinct steps, first a conversion to GDP, followed by a repositioning of GDP to further dephosphorylate it to GMP. Although GTP-GDP conversion has been shown to be sufficient for restricting pathogens such as *Chlamydia* (Xavier *et al.*, 2020), the second step and further degradation of GMP to urea is crucial for activation of the NLRP3 inflammasome (Schwemmle and Staeheli, 1994; Ghosh *et al.*, 2006).

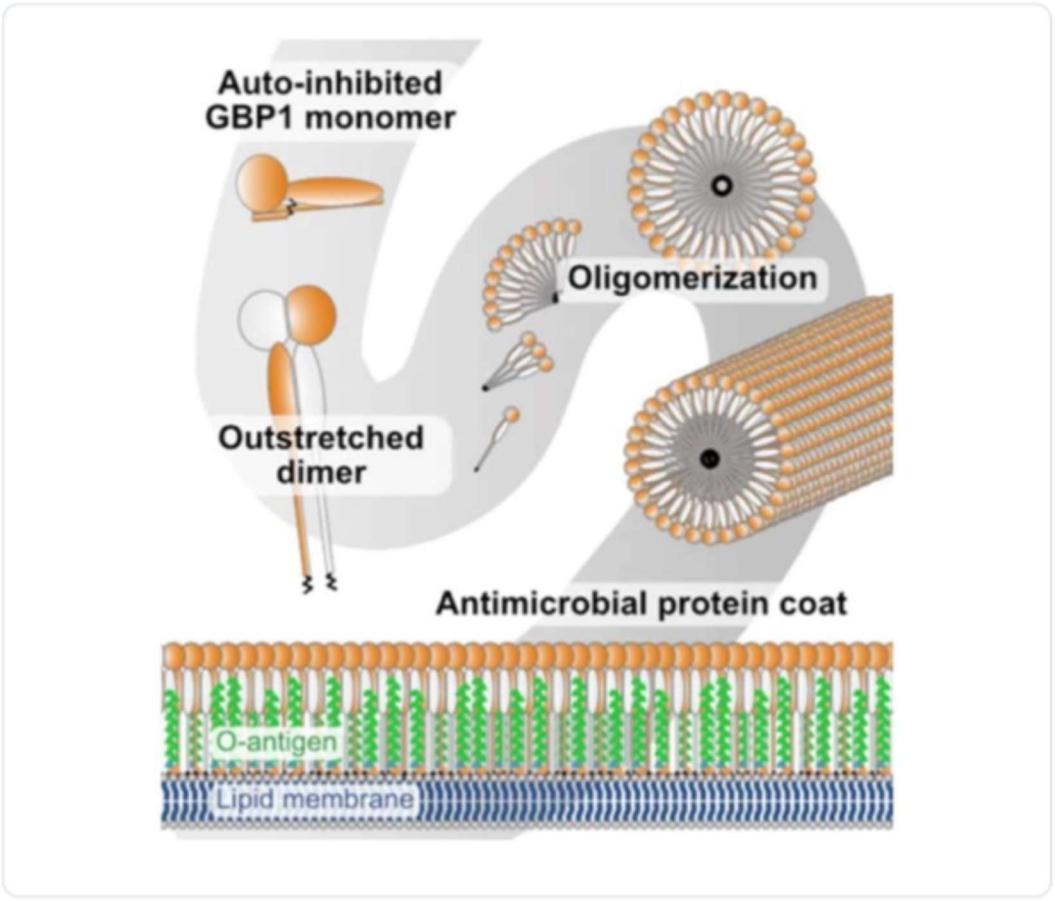

Figure 5 taken from (Weismehl *et al.*, 2024). Schematic depicting mechanism of formation of oligomeric GBP1 coat around bacterial outer membranes.

Upon activation, the GBP1 monomer dimerises into an outstretched conformation. This is followed by oligomerisation of multiple dimers into an oligomeric coat on the outer membrane of Gram-negative bacteria.

Other GBPs are also involved in the defence against intracellular pathogens. They are recruited to sites of infection in a hierarchical manner; GBP1 is recruited first, triggering the recruitment of other GBPs. In human epithelial cells, during *S.* typhimurium and *S. flexneri* infections, GBP1 is recruited to the surface of the bacterium, followed by GBP2 and GBP4, which are implicated in controlling the recruitment of caspase-4, and GBP3, which binds LPS and controls activation of caspase-4 (Wandel *et al.*, 2017, 2020; Santos *et al.*, 2020). *Shigella* effector IpaH9.8, an E3 ubiquitin ligase, ubiquitylates and marks the GBP coat for degradation, allowing for escape of the pathogen (Wandel *et al.*, 2017). GBP5 was the first GBP observed to contribute to inflammasome activation, through its interaction with NLRP3 (Shenoy *et al.*, 2012). However, the role of GBP5 in inflammation is not well-

characterised, and recent reports also indicate that it causes a decrease in pro-inflammatory secreted cytokines and chemokines (Li *et al.*, 2022). Surprisingly, the role of GBPs in extracellular-pathogen-induced pyroptosis remains unknown.

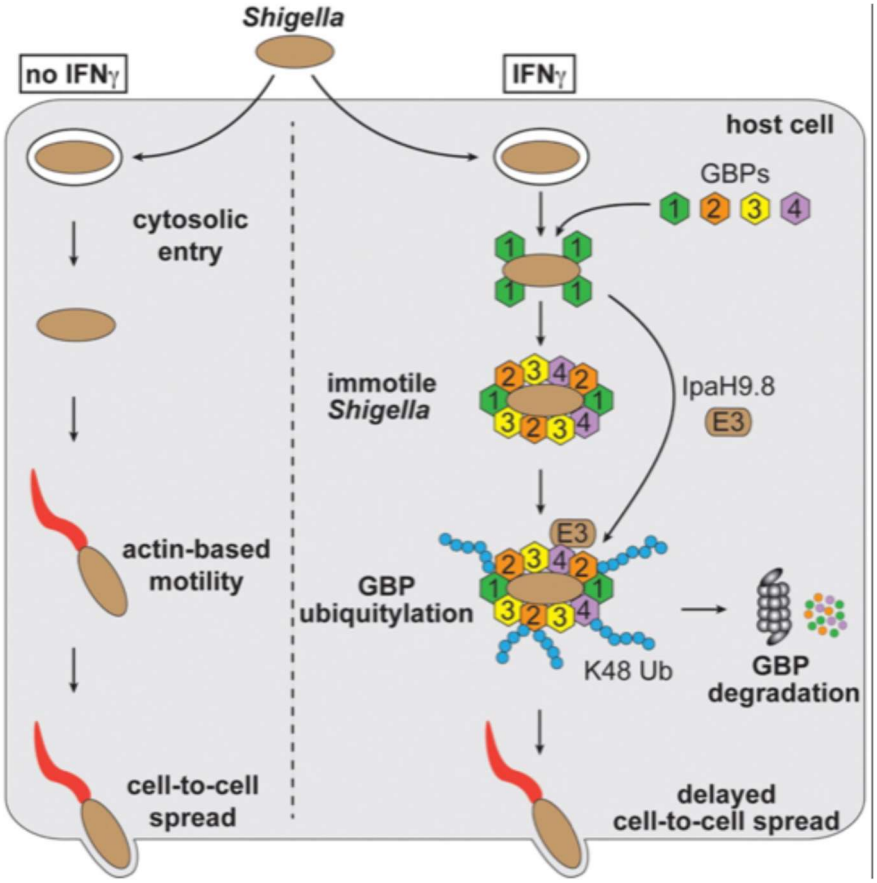

Figure 6 taken from (Wandel *et al.*, 2017). Schematic depicting the molecular steps involved in IFNγ-induced GBP coating of cytosolic *Shigella.*

Figure shows IFNγ-induced GBP coating of cytosolic *Shigella*, leading to delayed spread and helping control infection. Shigella effector IpaH9.8 ubiquitylates GBPs, allowing the pathogen to escape.

1.6. Extracellular pathogen-induced pyroptosis

Multiple studies have shown the role of GBPs as intracellular anti-microbial sensors of vacuolar or cytoplasmic pathogens, however their role in pyroptosis induced by extracellular A/E pathogens is not well-studied (Ceballos-Olvera *et al.*, 2011; Fisch *et al.*, 2019; Li *et al.*, 2020). EPEC induces caspase-4 mediated pyroptosis in macrophages through the NLRP3-caspase-1 inflammasome. EPEC is internalised by phagocytosis in THP-1 macrophages, allowing caspase-4 access to LPS, leading to its activation. Upon activation, caspase-4 activates the NLRP3-caspase-1

inflammasome, leading to proteolytic cleavage of pro-inflammatory cytokines and GSDMD, eventually resulting in pyroptosis. In the THP-1 infection system, the NLRP3-caspase-1 inflammasome is crucial for pyroptosis, as inhibiting NLRP3 led to a significant reduction in pyroptotic cell death (Goddard *et al.*, 2019).

Macrophages have two major limitations when used to model EPEC infections; They are phagocytic, hence they internalise EPEC inside the cell (Goddard *et al.*, 2019), which is not physiologically accurate, as A/E pathogens do not enter their host niche, the intestinal epithelia (Levine *et al.*, 1978). Another drawback is that they are immune cells and thus contain many immune pathways which are not present in intestinal epithelial cells (Smith *et al.*, 2005), thus it is important to assess infection by these pathogens in intestinal epithelial cell lines such as HT29 and CL40.

1.7. Scope of this study

In this study, we sought to understand the mechanisms involved in extracellular pathogen sensing by intracellular sensors such as GBP1 and caspase-4 during infection in intestinal epithelial cells. We also assessed the role of the NLRP3-caspase-1 inflammasome axis during pyroptosis in these cells, and whether it is dispensable. Caspase-4 has been implicated in defence against EPEC in macrophages (Goddard *et al.*, 2019); thus, we investigated its role in the immune response of intestinal epithelial cells against EPEC and EHEC, which are the natural physiological niches of these pathogens. We also investigated the role of GBPs in assisting caspase-4 in mounting an immune response to these pathogens, as has been previously reported with intracellular pathogens. Past work from Dr. Daniel Bennison in the Shenoy lab has shown that GBP1 is recruited to actin pedestals at sites of EPEC infection, so we sought to determine whether caspase-4 is also recruited to these pedestals (Bennison *et al.*, 2025) (Fig. 7 A). He also showed that pyroptosis is significantly reduced in GBP1$^{-/-}$ HeLa cells (Fig. 7 B), suggesting an important role for GBP1 in A/E-pathogen-induced pyroptosis. Finally, we dissected the mechanisms by which immune sensing occurs using an ingeniously designed “sterile” Tir-clustering system to assess the role of LPS during recruitment of these proteins to sites of infection and during pyroptosis.

A

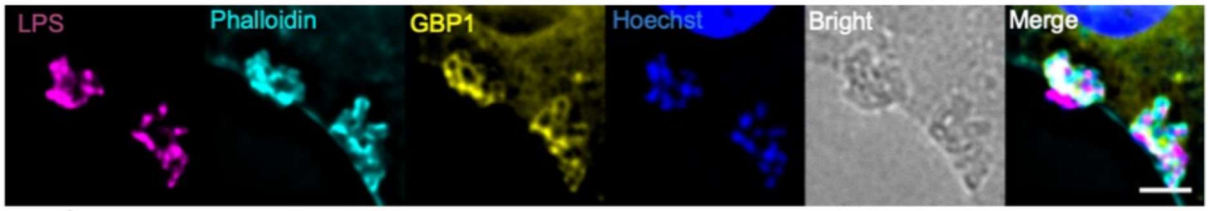

B

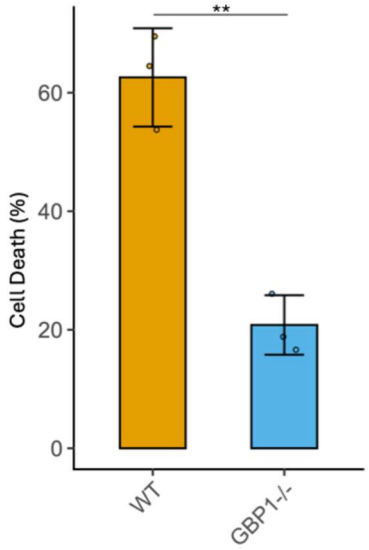

Figure 7: GBP1 is involved in immune responses to EPEC infections in HeLa cells

(A) Panel taken from (Bennison *et al.*, 2025). Representative immunofluorescence image of IFNγ-primed HeLa cells infected with EPEC for 2 hours followed by staining with anti-GBP1 mouse monoclonal antibody, Phalloidin-AlexaFluor-568 and Hoechst Dye to stain for nuclei.

(B) Percentage pyroptosis as measured by PI uptake assays in IFNγ-primed HeLa cells infected with EPEC for 6 hours. Mean ± SD is shown for data obtained from Dr. Daniel Bennison from n = 3 independent experiments. **P ≤ 0.01.

2. Materials and Methods

2.1. Materials

2.1.1. Table 1: Cell lines used in this study

Cell Line	Source
CL40	ATCC
CL40 pMXCMV-miR30E- CASP4	(Bennison *et al.*, 2025)
CL40 pMXCMV-miR30E- Ctrl	(Bennison *et al.*, 2025)
CL40 pMXCMV-miR30E- GBP1#3+8	(Bennison *et al.*, 2025)
CL40 pMXCMV-miR30E-GSDMD	(Bennison *et al.*, 2025)
HEK293E	(Eldridge *et al.*, 2017; Goddard *et al.*, 2019; Mishra *et al.*, 2023)
HeLa	ATCC
HeLa GBP1$^{-/-}$	(Bennison *et al.*, 2025)
HeLa GBP1$^{-/-}$ pMX- FcγRIIa-Tir-MYC	(Bennison *et al.*, 2025)
HeLa pMXCMV-miR30E- CASP4	(Bennison *et al.*, 2025)
HeLa pMXCMV-miR30E- Ctrl	(Bennison *et al.*, 2025)
HeLa pMXCMV-miR30E- GBP2#1+2	(Bennison *et al.*, 2025)
HeLa pMXCMV-miR30E- GSDMD	(Bennison *et al.*, 2025)
HeLa pMX-FcγRIIa-Tir-MYC	(Bennison *et al.*, 2025)
HT29	ATCC
HT29 pMXCMV-miR30E- CASP4	(Bennison *et al.*, 2025)
HT29 pMXCMV-miR30E- Ctrl	(Bennison *et al.*, 2025)
HT29 pMXCMV-miR30E- GBP1#3+8	(Bennison *et al.*, 2025)
HT29 pMXCMV-miR30E- GBP2#1+2	(Bennison *et al.*, 2025)

2.1.2. Table 2: Bacterial strains used in this study

Strain	Source	Identifier
EHEC 85-170	(Levine *et al.*, 1978)	O157:H7
EHEC 85-170 *Δeae*	(Bennison *et al.*, 2025)	O157:H7
EHEC 85-170 *ΔescN*	(Bennison *et al.*, 2025)	O157:H7
EHEC 85-170 *ΔtccP*	(Bennison *et al.*, 2025)	O157:H7
EHEC 85-170 *Δtir*	(Bennison *et al.*, 2025)	O157:H7
EPEC E2348/69	(Bennison *et al.*, 2025)	O127:H6
EPEC E2348/69 *Δeae*	(Marchès *et al.*, 2008)	O127:H6
EPEC E2348/69 *ΔescF*	(Wilson *et al.*, 2001)	O127:H6
EPEC E2348/69 *Δtir*	(Berger *et al.*, 2009)	O127:H6
Stbl2 E. coli	(Trinh, *et al.*, 1994)	-

2.1.3. Table 3: Plasmids used in this study

Plasmid	Source
pCMV-HIV-Gag-Pol (HIV-1266)	Walther Mothes
pCMV-MMLV 6 Walther Mothes	Walther Mothes
pCMV-VSV-G 6 Walther Mothes	Walther Mothes
pMXCMV-FcγRIIa-Tir-MYC	(Bennison *et al.*, 2025)
pMXCMV-YFP-CASP4^{C258S}	(Bennison *et al.*, 2025)
pMXCMV-YFP-miR30E- CASP4	(Bennison *et al.*, 2025)
pMXCMV-YFP-miR30E- Control	(Bennison *et al.*, 2025)
pMXCMV-YFP-miR30E- GBP1 #3	(Bennison *et al.*, 2025)
pMXCMV-YFP-miR30E- GBP1 #8	(Bennison *et al.*, 2025)
pMXCMV-YFP-miR30E- GBP2 #1	(Bennison *et al.*, 2025)
pMXCMV-YFP-miR30E- GBP2 #2	(Bennison *et al.*, 2025)
pMXCMV-YFP-miR30E- GSDMD	(Bennison *et al.*, 2025)
pTet-rtTA-tTS	(Fisch *et al.*, 2019)

2.1.4. Table 4: DNA constructs used in this study

Construct	Sequence	Source
CASP4 miR30E	ATATCTTGTCATGGACAGTCGT	(Bennison *et al.*, 2025)
CTRL miR30E	TCACGACGTTGTAATACGACGT	(Bennison *et al.*, 2025)
GBP1 miR30E#3	CAGGAACAGGAGCAACTACTAA	(Bennison *et al.*, 2025)
GBP1 miR30E#8	AGAACACTAATGGGCGACTGAT	(Bennison *et al.*, 2025)
GBP2 miR30E#1	TCAGGATATATTTGGCCCTTTA	(Bennison *et al.*, 2025)
GBP2 miR30E#2	AAAGGTACTGATAAGAAAAGTA	(Bennison *et al.*, 2025)
GSDMD miR30E	TACACATTCATTGAGGTGCTGG	(Bennison *et al.*, 2025)

2.2. Methods

2.2.1. Cell culture

Cell lines were cultured in a humidified incubator at 5% CO_2 and at 37 °C. HeLa and HEK cell lines were grown in Dulbecco's Modified Eagle's Medium (DMEM) supplemented with sodium pyruvate (1 mM), penicillin (100 units/mL), streptomycin (100 units/mL), and 10% heat-inactivated Foetal Bovine Serum (HI-FBS). CL40 cell lines were cultured in DMEM/Ham's F12, supplemented with sodium pyruvate (1 mM), penicillin (100 units/mL), streptomycin (100 units/mL), and 20% HI-FBS. Additionally, Zeosin (200 µg/mL), Blasticidin S (10 µg/mL), or Puromycin (2 µg/mL) were added when required for the appropriate cell lines. Doxycycline (200 ng/mL) was added overnight before experiments where pTet-rtTA-tTS plasmid expression was required.

2.2.2. Bacterial culture

EPEC strains were grown in 5 mL Luria Bertani Broth (LB) overnight in a shaking incubator at 37 °C followed by diluting 1:50 in low-glucose DMEM and left standing in a humidified incubator with 5 % CO_2 for 3 h to allow bacterial priming and expression of the LEE regulon. EHEC strains were grown for 8 hours in LB in a shaking incubator at 37 °C followed by overnight priming 1:50 in low-glucose DMEM. Kanamycin was added at a concentration of 30 µg/mL for appropriate knockout strains.

2.2.3. Generation of GBP2 knockout HeLa cells

HeLa cells were plated in a 24-well plate at a density of 10^5 cells/well. The next day they were co-transfected with 125 ng each of plasmids expressing *Sp*Cas9 and GBP2-specific gRNA using TransIT-X2 Dynamic Delivery System (Mirus) according to the manufacturer's instructions with transfection complexes prepared in OptiMEM. Plasmids containing two gRNA targeting the entire coding sequence of GBP2 were cotransfected into HeLa cells. After 48 h post-transfection, untransfected cells were killed by culturing in puromycin (2 µg/mL). After 72 hours of puromycin selection, surviving cells were trypsinised and diluted to a concentration of ~3 cell/mL and plated in two 10 cm dishes to obtain single-cell clones. After culturing for ~3 weeks, clones were picked up using sterile filter paper discs dipped in trypsin-EDTA solution. Discs containing cells were shaken in one well of a 48-well plate (containing 250 µL media) to release loosely attached cells and the disc was placed with the face containing adherent cells facing up in a second 48-well (2 wells per clone). When these wells were confluent, cells were passaged to 12-well plates. Screening of clones was carried out using Western blotting to assess GBP2 protein expression.

2.2.4. Gene silencing with miRNA30E

To knock down GBP1, GBP2, Caspase-4 and GSDMD, gene-specific 22-base oligonucleotides were designed and cloned into the pMX-CMV-eYFP-miR30E backbone at XhoI and EcoRI restriction sites. Sequences used are listed in Table 4. The silencing plasmids were then transduced into HeLa, HT29 and CL40 cell lines to create stable silenced cell lines. Silencing was confirmed using Western blot analysis of protein expression.

2.2.5. Molecular Cloning and Protein Expression

Cloning was carried out using Sequence Ligase Independent Cloning (SLIC). The 22-base oligonucleotide insert was amplified using PCR and the plasmid backbone was digested using EcoRI and XhoI restriction enzymes. The insert and backbone were ligated using the T4 exonuclease-based ligase-independent method (Jeong *et al.*, 2012). 100 ng of backbone and 4x molar ratio of insert were mixed along with T4 polymerase (0.2 µL) and 10x NEB rCutSmart™ buffer in a 20 µL reaction. Upon adding polymerase, the reaction mixture was kept at room temperature for exactly 2.5 minutes followed by ice for 10 minutes to stop exonuclease activity. Half of the

reaction mixture was then transformed into Stbl2 E. coli competent cells and selected on Luria Bertani agar plates containing ampicillin (100 µg/mL). The next day, plasmids were mini-prepped from the resultant colonies and screened using restriction digestion followed by confirmation with Sanger Sequencing. GBP2,3,4 and 5 were overexpressed using Doxycycline-inducible pTetDF-mCh vector along with the control vector pTet-rtTA-tTS.

2.2.6. Retroviral and Lentiviral Packaging and Transduction

HEK293E cells were plated in a 24-well format at a density of 1 x 10^5 cells/well. The next day, retroviral plasmids (pMX backbone) and pCMV-MMLV-Gag-Pol or lentiviral plasmids (pTet backbone) and pHIV-1266 were co-transfected along with pCMV-VSV-G-Env into the plated cells in a ratio of 5:4:1 for pMX-plasmid:Gag-Pol:VSV-G (for retroviral plasmids) or 3:2:1 pTet-plasmid:HIV-1266:VSV-G (for lentiviral plasmids). At 48 hours post transfection, HEPES (10 mM) was added to the supernatant to stabilize pH and virus-containing supernatant was harvested and filter-sterilised through 0.45 µm filters. Recipient cells were plated in a 24-well format and 250 – 400 µL of filtered supernatant was added to transduce the plasmid of interest. At 48 hours post transduction, the appropriate selection antibiotic was added to select for transduced cells.

2.2.7. Cell Death Assays

HeLa, HT29 and CL40 cell lines were plated at 4 x 10^4 cells/well (HeLa), 7 x 10^4 cells/well (HT29), or 1.4 x 10^5 cells/well (CL40) in rows in 96-well plates. The next day, medium was changed to DMEM (-) medium which is the culture medium used above but without penicillin, streptomycin, and phenol red. IFNγ (10 ng/mL) was added to the medium to prime the cells overnight. Primed bacterial cultures were diluted in low-glucose DMEM to the appropriate Multiplicity of Infection (MOI) and cells were infected with EPEC cultures at MOI 30 for 2 hours or with EHEC at MOI 50 for 5 hours followed by gentamicin (200 µg/mL) addition to kill excess bacteria. At the start of the infection, along with bacteria, Propidium Iodide (PI) was added (5 µg/mL) to all wells along with one row of cells where 0.05 % Triton-X was added as a positive control, and one row of cells which were left uninfected as a negative control. Cell death in experimental groups was normalised (as percentage) cell death with respect to the positive after removing the value of uninfected negative control

wells. PI fluorescence was measured from 2 hours post infection up to 6 hours or 18 - 24 hours at intervals of 15 minutes.

2.2.8. Immunofluorescence Microscopy

Slide Preparation

HeLa and HT29 cell lines were plated at a density of 1 x 10^5 cells/well on cover slips in 24-well plates. The next day, cells were primed with IFNγ (10 ng/mL) overnight. Primed bacterial cultures were diluted to the appropriate Multiplicity of Infection and cells were infected with EPEC cultures at MoI 5 for 3 hours or with EHEC at MoI 20 for 5 hours. Cells were then washed twice with PBS followed by fixation in 4% paraformaldehyde (PFA) prepared in PBS for 20 minutes with the plate wrapped under aluminium foil to avoid light exposure. The cells were then again washed twice with PBS for 5 minutes each followed by quenching of the PFA with 50 mM ammonium chloride solution in PBS for 20 minutes. Cells were then stored in PBS at 4 ^oC for further processing.

For staining, all antibodies were diluted in 5% donkey serum and 0.1% saponin prepared in PBS. Fixed cells were stained with anti-GBP1 (1:500) mouse monoclonal antibody and Phalloidin-AlexaFluor568 (1:400) overnight, followed by secondary staining with anti-mouse-AlexaFluor647 (1:1000) secondary antibody and Hoechst DNA dye (1:500) to visualise bacteria and nuclei for 1 h at room temperature. YFP-Caspase-4^{C258S} emits at a wavelength of 524 nm and was not stained with antibodies.

For FLAG-tagged GBP2,3 and 5, the proteins were visualised using anti-FLAG (1:400) mouse monoclonal antibody followed by anti-mouse-AlexaFluor647 secondary antibody and Hoechst DNA dye as above. For MYC-tagged GBP4, anti-MYC (1:400) mouse monoclonal antibody was used.

After secondary antibody treatment, cover slips were washed and mounted on slides with Invitrogen ProLong™ Diamond Antifade Mountant and left to cure overnight in darkness at room temperature.

Image acquisition and processing

Images were acquired using a Zeiss CellDiscoverer 7 epifluorescence microscope fitted with an Axiocam 504 mono camera and a Colibri.2 light source. PApo 50x/1.2

water auto-immersion lens along with an afocal magnification lens at 2x magnification were used to acquire images at 100x magnification. LEDs of wavelengths of 385, 470, 520, 567, 590, 625 nm were used along with Zeiss 90 HE, 91 HE and 92 HE filter sets. Raw images were deconvolved and processed using Fiji ImageJ software. Point Spread Functions (PSFs) were generated for each wavelength using the PSFGenerator ImageJ plugin available (Kirshner *et al.*, 2013). Deconvolution was performed using 25 iterations of the Richardson-Lucy method using the DeconvolutionLab2 ImageJ plugin (Sage *et al.*, 2017).

2.2.9. IgG Bead Preparation and Treatment

Bead Preparation

Spherotech SPHERO™ Polystyrene Particles (3.54 µm diameter beads) were coated with either BSA or human immunoglobulin G (IgG). Beads were washed twice with PBS and spun down at 5,000 x*g* followed by sterilisation in 100% ethanol for 10 minutes. They were again washed thrice in PBS and then treated with a solution of 500 µg/mL of BSA or 500 µg/mL of human IgG overnight on a rotating wheel at 10 rpm at 4 ^{o}C. The next day, the beads were washed twice with sterile PBS and counted using a haemocytometer.

Bead Treatment

HeLa WT or *GBP1*$^{-/-}$ cells expressing FcγR-Tir chimeric receptors were treated with IgG or BSA (negative control) - coated beads at a multiplicity of 5 beads:1 cell for 15 minutes, followed by washing with DMEM to remove excess beads. The medium was changed to OptiMEM, and cells incubated at 37 ^{o}C and 5% CO_2 in a humidified incubator for 3 hours, followed by fixing with PFA for immunofluorescence experiments as described above. For cell death assays, cells were incubated in OptiMEM containing PI (5 µg/mL) for 24 hours with measurements taken every 15 minutes as described above.

2.2.10. Western Blot Analysis

HeLa, HT29 and CL40 cell lines were grown in 48-well plates to confluency. The cells were then washed once with ice-cold PBS and lysed in 100 mL of RIPA buffer (60 mM Tris (pH 8.0), 150 mM NaCl, 1% NP-40, 0.5% Na-deoxycholate, 1 mM EDTA) supplemented with Pierce™ protease inhibitor and 1 mM

phenylmethylsulfonyl fluoride (PMSF). Samples were mixed with Laemmli loading dye containing 5 % β-mercaptoethanol and proteins separated on a 10 % SDS-PAGE at 100 V for 12 minutes followed by 200 V for 45 minutes. The proteins were transferred onto a PVDF membrane using a semi-dry transfer method in 1X Transblot buffer (1.21g Trizma base, 7.5g Glycine, 100 mL methanol in 1L solution) for 30 minutes at 25 V. The membrane was blocked using 5 % skim milk prepared in PBST for 1 hour and primary antibody treatment overnight at 4 ^{o}C. All antibodies were diluted in 5% Bovine Serum Albumin (BSA) in PBST and used at a dilution of 1:1000, except GBP1 mouse monoclonal used at 1:2000. The next day, membranes were washed 3 times in PBS for 15 min each, treated with anti-mouse or anti-rabbit secondary antibodies (1:20,000) diluted in 5% skim milk fused with Horse-Radish Peroxidase for 1 hour and developed using BioRad Clarity™ Western ECL Substrate to visualise the proteins of interest. All the steps were separated by membrane washes in 1x PBST (PBS + 0.1 % Tween-20).

2.2.11. Data Analyses

For all experiments, two technical replicates from adjacent wells in a 96-well plate were averaged to calculate a single mean value. Independent biological replicates refer to experiments performed with distinct passages of cell lines and freshly inoculated bacterial cultures on separate days. Data were organized in MS Excel and analysed and plotted in R (v.4.0 or higher) using grafify, ggplot2, readxl, dplyr and tidyr packages. Mean and standard deviation (SD) are displayed for bar graphs.

Statistical comparisons were made using one-way ANOVA of mixed effects linear models fitted with random factors (experiments) and fixed factors. Studentised residuals were plotted as Quantile-Quantile plots to ensure normal distribution.

3. Results

3.1. CASP4 and GSDMD silencing reduces EPEC-induced pyroptosis

Previous studies have shown that Caspase-4 and GSDMD are involved in the pyroptosis pathway during infections of epithelial cells with Gram-negative intracellular pathogens such as *Salmonella* (Fisch *et al.*, 2019). To test whether this is also true in the case of extracellular pathogen infections in intestinal epithelial cells, caspase-4 and GSDMD were silenced in HeLa, CL40 and HT29 cell lines using miRNA30E constructs and protein expression in the silenced cell lines was assessed using western blot analysis.

Upon confirming successful silencing (Fig. 8 D-F), the silenced cell lines were infected with EPEC for 6 or 12 hours and pyroptotic cell death was measured using PI fluorescence. We observed a significant reduction in pyroptotic cell death in cell lines where either caspase-4 or GSDMD was silenced, suggesting that these proteins play an important role in pyroptosis in human intestinal epithelial cells lines and HeLa cells upon EPEC infection (Fig. 8 A-C).

A portion of the results described in this section have been published as a pre-print (Bennison et. al., 2025), which may lead to high similarity in parts.

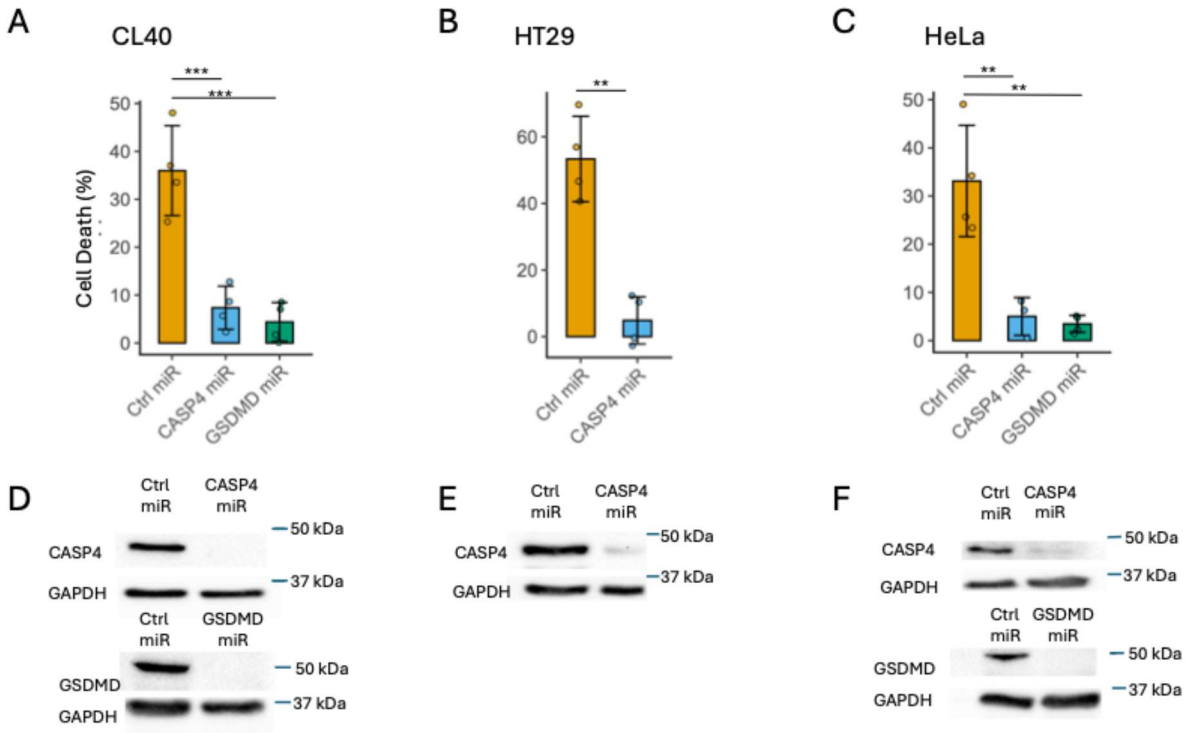

Figure 8: CASP4 and GSDMD silencing lead to reduced pyroptosis upon EPEC infection

(A) Percentage pyroptosis as measured by PI uptake assays of IFNγ-treated CL40 cell lines silenced for Caspase-4 or GSDMD or transduced with a control miRNA30E as a control infected with EPEC. Measurements were plotted at 6 hours post infection. Mean ± SD from n = 4 independent experiments are depicted.

(B) Percentage pyroptosis as measured by PI uptake assays of IFNγ-treated HT29 cell lines silenced for Caspase-4 or transduced with a control miRNA30E as a control infected with EPEC. Measurements were plotted at 12 hours post infection. Mean ± SD from n = 4 independent experiments are depicted.

(C) Percentage pyroptosis as measured by PI uptake assays of IFNγ-treated HeLa cell lines silenced for Caspase-4 or GSDMD or transduced with a control miRNA30E as a control infected with EPEC. Measurements were plotted at 6 hours post infection. Mean ± SD from n = 3 independent experiments are depicted for HeLa CASP4 and GSDMD miR30E cell lines and n = 4 for Ctrl miR30E cell line.

(D) Representative Western blots showing silencing of Caspase-4 and GSDMD in cell lysates of IFNγ-treated CL40 cells stably expressing the non-targeting control (Ctrl) or the indicated miR30E. GAPDH was used as a loading control. Blots are representative of n = 3 independent experiments.

A portion of the results described in this section have been published as a pre-print (Bennison et. al., 2025), which may lead to high similarity in parts.

(E) Representative Western blots showing silencing of Caspase-4 in cell lysates of IFNγ-treated HT29 cells stably expressing the non-targeting control (Ctrl) or Caspase-4 miR30E. GAPDH was used as a loading control. Blots are representative of n = 3 independent experiments.

(F) Representative Western blots showing silencing of Caspase-4 and GSDMD in cell lysates of IFNγ-treated HeLa cells stably expressing the non-targeting control (Ctrl) or the indicated miR30E. GAPDH was used as a loading control. Blots are representative of n = 3 independent experiments.

Data Information: **P ≤ 0.01, ***P ≤ 0.001 for indicated comparisons in panels A-C from one-way mixed model ANOVA.

3.2. GBP1-silencing in intestinal epithelial cells reduces EPEC-induced pyroptosis

Previous data from the lab showed that pyroptosis is significantly reduced in IFNγ-primed GBP1 knockout HeLa cells upon EPEC infection (Bennison *et al.*, 2025). To assess the role of GBP1 in physiologically relevant intestinal epithelial cells, GBP1 was silenced in CL40 and HT29 using miR30E-based stable silencing.

We achieved partial silencing of GBP1 (Fig. 9 C,D) and observed that upon IFNγ induction in these cells, there was significant reduction in pyroptosis (Fig. 9 A,B).

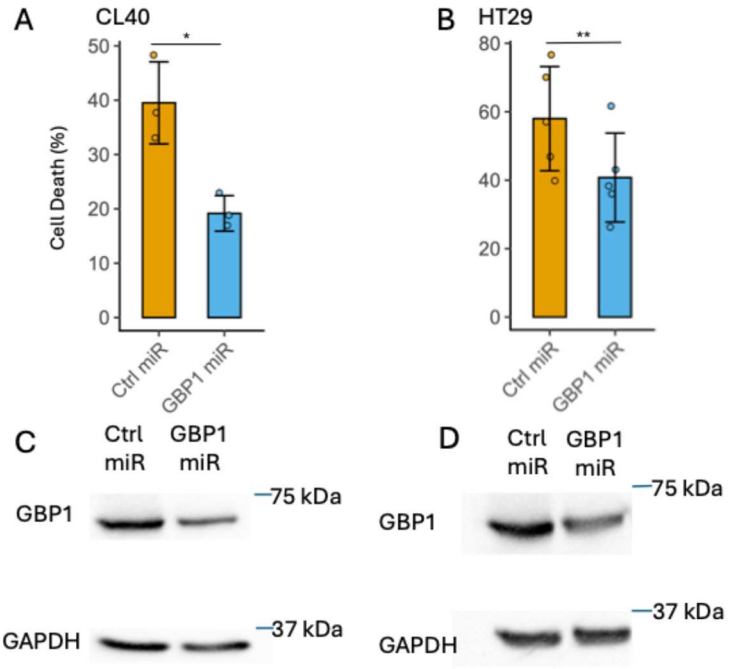

A portion of the results described in this section have been published as a pre-print (Bennison et. al., 2025), which may lead to high similarity in parts.

Figure 9: Partial GBP1 silencing in intestinal epithelial cells leads to reduction in pyroptosis.

(A) Percentage pyroptosis as measured by PI uptake assays of IFNγ-treated CL40 cell lines silenced for GBP1 or transduced with a control miRNA30E as a control infected with EPEC. Measurements were plotted at 6 hours post infection. Mean ± SD from n = 3 independent experiments are depicted.

(B) Percentage pyroptosis as measured by PI uptake assays of IFNγ-treated HT29 cell lines silenced for GBP1 or transduced with a control miRNA30E as a control infected with EPEC. Measurements were plotted at 12 hours post infection. Mean ± SD from n = 5 independent experiments are depicted. Four independent replicates were performed by Ayush Punwatkar.

(C) Representative Western blots showing silencing of GBP1 in cell lysates of IFNγ-treated CL40 cells stably expressing the non-targeting control (Ctrl) or GBP1 miR30E. GAPDH was used as a loading control. Blots are representative of n = 3 independent experiments.

(D) Representative Western blots showing silencing of GBP1 in cell lysates of IFNγ-treated HT29 cells stably expressing the non-targeting control (Ctrl) or GBP1 miR30E. GAPDH was used as a loading control. Blots are representative of n = 3 independent experiments.

Data Information: *P ≤ 0.05, **P ≤ 0.01 for indicated comparisons in panels A-C from one-way mixed model ANOVA.

3.3. GBP2 localises in the vicinity of actin pedestals but GBP3,4 and 5 do not.

Upon observing the role of GBP1 in IFNγ-primed cells upon EPEC infection, we further assessed whether the other GBPs have a role to play in this process. Past reports on innate immune response to *Salmonella sp.* have shown that GBP 2 and 5 may also play accessory roles alongside GBP1 in LPS detection and triggering pyroptosis (Shenoy *et al.*, 2012; Santos *et al.*, 2020).

Thus, FLAG-GBP2 was transfected into HeLa cells or transduced and expressed in a Doxycycline-inducible manner, as constitutive expression of GBPs is lethal to cells. We observed that FLAG-GBP2 weakly localised in the vicinity of actin pedestals (Fig. 10). It was not present at every actin pedestal in the same manner as GBP1 at 3 hours post infection.

A portion of the results described in this section have been published as a pre-print (Bennison et. al., 2025), which may lead to high similarity in parts.

Further, we transfected FLAG-GBP3, FLAG-GBP5 and MYC-GBP4 into HeLa cells in a similar manner to GBP2. We observed that these proteins did not get recruited to actin pedestals (Fig. 10) and thus we hypothesised that they may play little to no role in pyroptosis. Further experiments were not conducted with these GBPs.

Weaker recruitment of GBP2 suggested that it may not be as crucial to pyroptosis as GBP1. Hence, we proceeded to test for pyroptosis in GBP2-silenced cell lines through PI-based cell death assays.

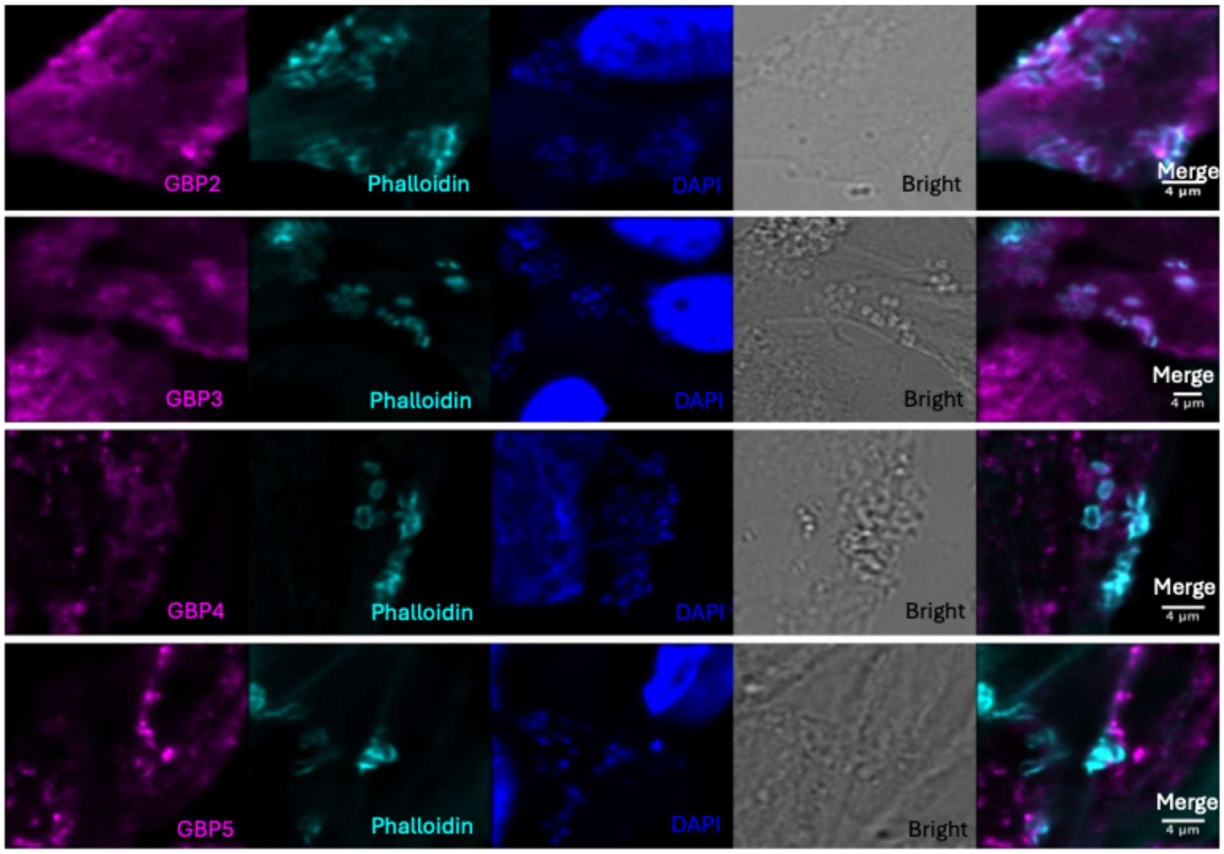

Figure 10: GBP2 is intermittently recruited to actin pedestals but GBP3,4 and 5 are not.

Representative immunofluorescence image of HeLa cells transfected with 3XFLAG-tagged GBP2,3 or 5 or MYC-tagged GBP4 upon IFNγ priming and infected with EPEC WT for 3 hours. Images are representative of n = 3 independent experiments. Cells were stained with FLAG-AlexaFluor647 to visualise GBP2-FLAG, Phalloidin-AlexaFluor568 to visualise actin and Hoechst Dye to visualise nuclei.

A portion of the results described in this section have been published as a pre-print (Bennison et. al., 2025), which may lead to high similarity in parts.

3.4. GBP2 silencing does not affect EPEC-induced pyroptosis in epithelial cells

To assess the effect of loss of GBP2 on EPEC-induced pyroptosis, we attempted to create GBP2 knockouts in HeLa cell lines using CRISPR-Cas9 as described in Methods. Although we were successful in creating knockouts, CRISPR-Cas9 knockouts can often have clone-dependent effects, thus to minimize these effects we pooled clone three knockout lines, HeLa GBP2$^{-/-}$ #5,9,10 to make HeLa GBP2$^{-/-}$ pooled cell line and three wild type (WT) lines, HeLa WT #1,2,6 to make HeLa WT pooled cell line.

Unexpectedly, the GBP2 knockout appeared to have off-targets effect and the GBP2$^{-/-}$ pool also had suppressed GBP1 expression (Fig. 11 B). Therefore, we could not attribute the reduction in pyroptosis observed (Fig. 11 A) to the GBP2 knockout alone, as the phenotype copies that of HeLa GBP1$^{-/-}$ cells.

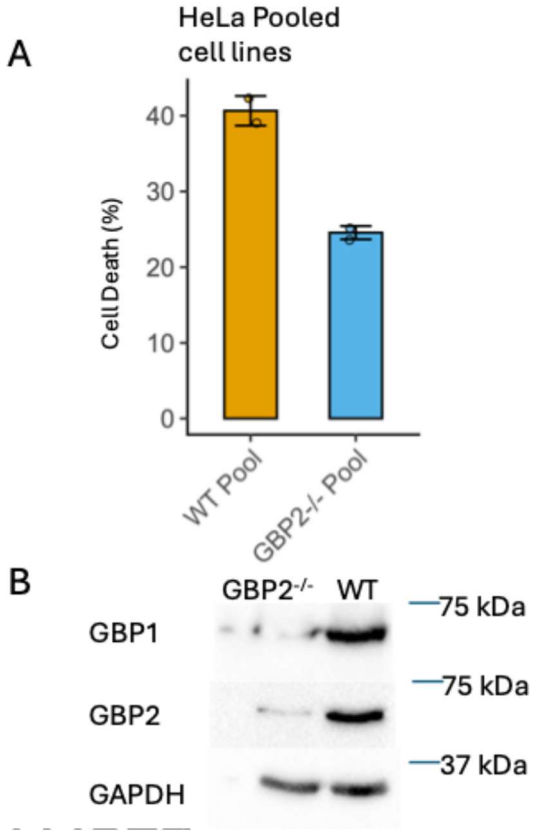

A portion of the results described in this section have been published as a pre-print (Bennison et. al., 2025), which may lead to high similarity in parts.

Figure 11: HeLa GBP2$^{-/-}$ pooled cell lines have impaired GBP1 expression. GBP2$^{-/-}$ lines created by Dr. Avinash Shenoy.

(A) Percentage pyroptosis as measured by PI uptake assays of IFNγ-treated HeLa GBP2$^{-/-}$ pooled (HeLa GBP2$^{-/-}$ #5,9,10) or HeLa WT pooled (HeLa WT #1,2,6) cell lines infected with EPEC. Measurements were plotted at 12 hours post infection due to delayed pyroptotic response in these cell lines. Mean ± SD from n = 2 independent experiments are depicted.

(B) Representative Western blots showing GBP1 and GBP2 expression in cell lysates of IFNγ-treated HeLa GBP2$^{-/-}$ pooled (HeLa GBP2$^{-/-}$ #5,9,10) or WT HeLa pooled (HeLa WT #1,2,6) cell lines. GAPDH was used as a loading control. The immunoblot was only conducted n = 1 time.

Statistical analysis was not carried out for these experiments as sufficient replicates were not conducted.

To resolve this issue, we instead proceeded with GBP2 silencing in HeLa and HT29 cell lines by stable transduction of GBP2 miR30E plasmids #1 and 2 (see Methods). Upon successful GBP2 silencing (Fig.12 C,D), we observed no significant difference in pyroptosis in GBP2-silenced cells as compared to cells treated with the Control miRNA30E (Fig. 12 A,B), indicating that GBP2 does not play a major role in IFNγ-induced pyroptosis upon EPEC infection.

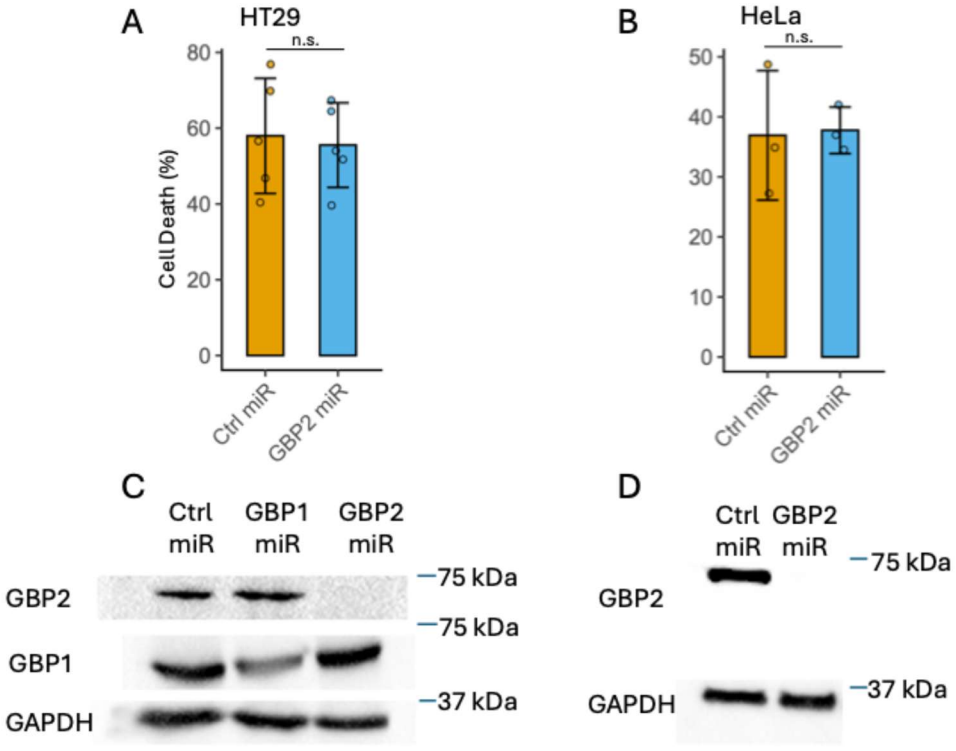

A portion of the results described in this section have been published as a pre-print (Bennison et. al., 2025), which may lead to high similarity in parts.

Figure 12: GBP2 silencing does not affect pyroptosis in intestinal epithelial cells. GBP2 miRNA constructs were created by Ayush Punwatkar and Miyu Stephenson.

(A) Percentage pyroptosis as measured by PI uptake assays of IFNγ-treated HT29 cell lines silenced for GBP2 or transduced with a control miRNA30E as a control infected with EPEC. Measurements were plotted at 12 hours post infection. Mean ± SD from n = 5 independent experiments are depicted.

(B) Percentage pyroptosis as measured by PI uptake assays of IFNγ-treated HeLa cell lines silenced for GBP2 or transduced with a control miRNA30E as a control infected with EPEC. Measurements were plotted at 6 hours post infection. Mean ± SD from n = 3 independent experiments are depicted.

(C) Representative Western blots showing silencing of GBP2 in cell lysates of IFNγ-treated HT29 cells stably expressing the non-targeting control (Ctrl) or the indicated miR30E. GBP1 blots were conducted to verify no cross-reactivity between GBP1 and GBP2 miRNAs. GAPDH was used as a loading control. Blots are representative of n = 3 independent experiments.

(D) Representative Western blots showing silencing of GBP2 in cell lysates of IFNγ-treated HeLa cells stably expressing the non-targeting control (Ctrl) or GBP2 miR30E. GAPDH was used as a loading control. Blots are representative of n = 3 independent experiments.

Data Information: P > 0.05 was evaluated for indicated comparisons in panels A and B from one-way mixed model ANOVA. n.s. = not significant.

3.5. Caspase-4 is recruited to actin pedestals in a GBP-1-dependent manner

GBP1 and caspase-4 play a crucial role in detecting LPS during intracellular bacterial infections in macrophages and epithelial cells by trafficking to sites of infection, detecting LPS and initiating pyroptosis (Fisch *et al.*, 2019; Goddard *et al.*, 2019). Past work from our lab has also shown that GBP1 is recruited to actin pedestals upon EPEC infection (Bennison *et al.*, 2025).

To test whether caspase-4 is also recruited to these actin pedestals, EPEC or EHEC were used to infect IFNγ-primed HeLa cells expressing a catalytically inactive caspase-4 mutant fused with a YFP protein (HeLa WT YFP-Casp-4^{C258S}) or $GBP1^{-/-}$ cells expressing the same protein (HeLa $GBP1^{-/-}$ YFP-Casp-4^{C258S}). We observed that caspase-4 is recruited to actin pedestals in a GBP-1-dependent manner (Fig.

A portion of the results described in this section have been published as a pre-print (Bennison et. al., 2025), which may lead to high similarity in parts.

13), as caspase-4 recruitment to pedestals was greatly impaired in HeLa GBP1$^{-/-}$ YFP-Casp-4^{C258S} cells.

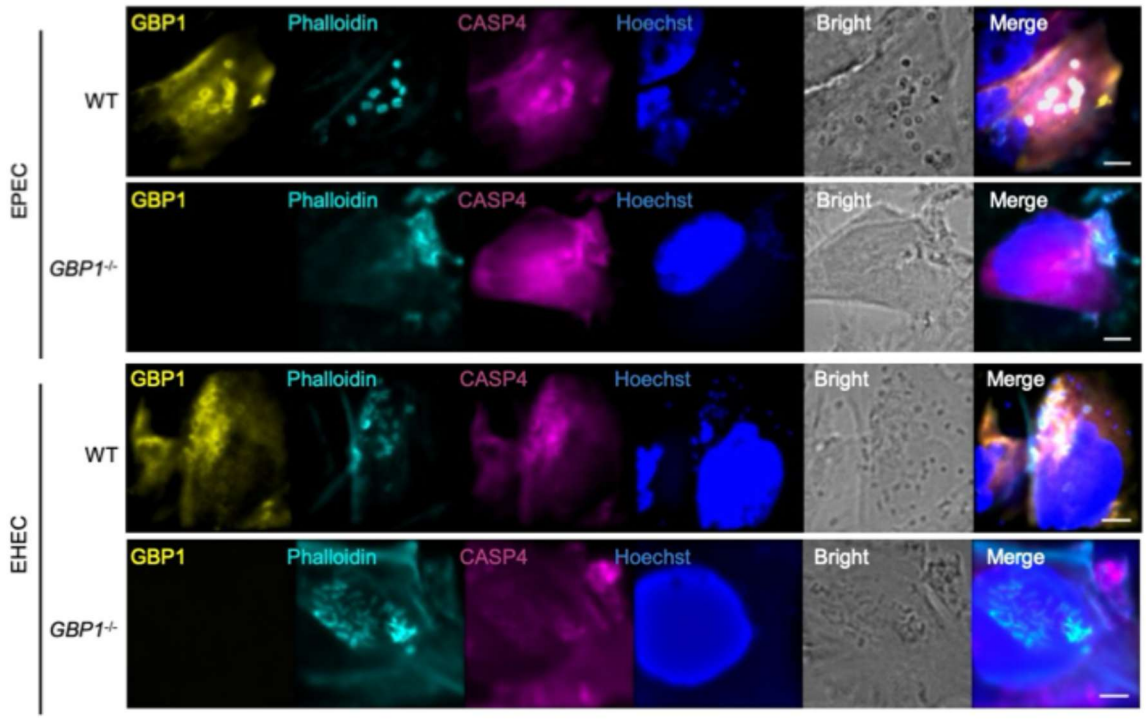

Figure 13: Caspase-4 is recruited to actin pedestals in a GBP1-dependent manner.

Representative immunofluorescence image of HeLa WT YFP-Casp-4^{C258S} or HeLa WT YFP-Casp-4^{C258S} cells infected with EPEC WT for 3 hours or EHEC WT for 5 hours. Images are representative of n = 3 independent experiments. Cells were stained with GBP1-AlexaFluor647 to visualise GBP1, Phalloidin-AlexaFluor568 to visualise actin and Hoechst Dye to visualise nuclei. Deconvolution and figure preparation was done by Dr. Avinash Shenoy. Scale bar = 4 µm.

3.6. EPEC-induced pyroptosis in epithelial cells is independent of NLRP3

In THP-1 macrophages, EPEC-induced pyroptosis is mediated by caspase4-NLRP3-caspase-1 signalling, where caspase-1 drives pyroptosis upon LPS-sensing by caspase-4(Goddard *et al.*, 2019). However, caspase-4 can also directly cleave GSDMD to initiate pyroptosis upon LPS detection (Fisch *et al.*, 2019). It is not clear which of these mechanisms is responsible for pyroptotic cell death in epithelial cells upon A/E pathogen infection.

A portion of the results described in this section have been published as a pre-print (Bennison et. al., 2025), which may lead to high similarity in parts.

To assess the involvement of the NLRP3-caspase-1 inflammasome axis during pyroptosis in epithelial cells, IFNγ-primed HeLa and HT29 cell lines were treated with the NLRP3 inhibitor MCC950 (10 µM) 30 minutes before the infection. This treatment has been successfully shown in previous experiments to reduce NLRP3-mediated pyroptosis in macrophage cell lines (Goddard *et al.*, 2019). However, we observed no reduction in pyroptosis in epithelial cells upon MCC950 treatment (Fig. 14 A,B), thus suggesting that NLRP-3 has no role in pyroptosis in epithelial cell lines upon EPEC infection and caspase-4-mediated GSDMD cleavage is the most likely mechanism of action for pyroptotic signalling.

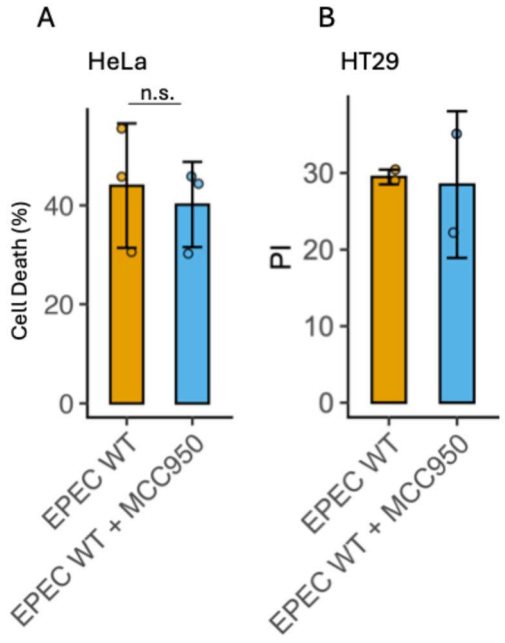

Figure 14: EPEC-induced pyroptosis in epithelial cells is independent of NLRP3.

(A) Percentage pyroptosis as measured by PI uptake assays of IFNγ-treated HeLa WT cells treated with the NLRP3 inhibitor MCC950 and infected with EPEC. Measurements were plotted at 6 hours post infection. Mean ± SD from n = 3 independent experiments are depicted.

(B) Percentage pyroptosis as measured by PI uptake assays of IFNγ-treated HT29 WT cells treated with the NLRP3 inhibitor MCC950 and infected with EPEC. Measurements were plotted at 12 hours post infection. Mean ± SD from n = 3 independent experiments are depicted.

Data Information: P > 0.05 was evaluated for indicated comparisons in panel A from one-way mixed model ANOVA. Statistical analysis was not carried out for panel B as sufficient replicates were not conducted. n.s. = not significant.

A portion of the results described in this section have been published as a pre-print (Bennison et. al., 2025), which may lead to high similarity in parts.

3.7. Pathogen-induced actin polymerisation is necessary for GBP1 and caspase-4 recruitment and pyroptosis

During *Salmonella* infections, GBP1 assists caspase-4 in LPS detection in the cytosol (Fisch *et al.*, 2019). However, since EPEC and EHEC are extracellular pathogens, it is not clear how GBP1 detects these pathogens to trigger pyroptotic responses.

To investigate this, HeLa cells were infected with EPEC and EHEC mutants which lack either a functional Type-3 Secretion System (T3SS) or effectors necessary for actin pedestal formation. EPEC *ΔescF* and EHEC *ΔescN* lack a functional T3SS, EPEC and EHEC *Δtir* lack the translocated intimin receptor (tir) required for actin pedestal formation, EPEC and EHEC *Δeae* lack intimin and EHEC *ΔtccP* lacks the tir-cytoskeleton coupling protein(tccP). We observed that no GBP1 or Caspase-4 recruitment occurs in the absence of actin pedestals (Fig. 15 A,B), thus indicating that actin pedestal formation is necessary for GBP1 and Caspase-4 recruitment to sites of infection

A portion of the results described in this section have been published as a pre-print (Bennison et. al., 2025), which may lead to high similarity in parts.

A

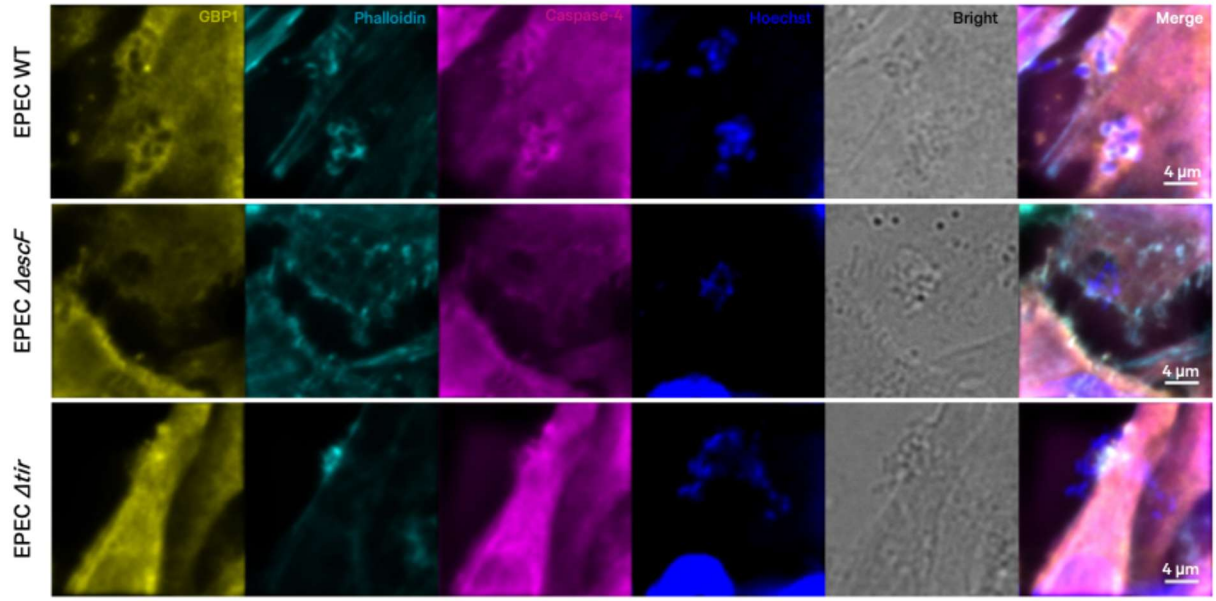

B

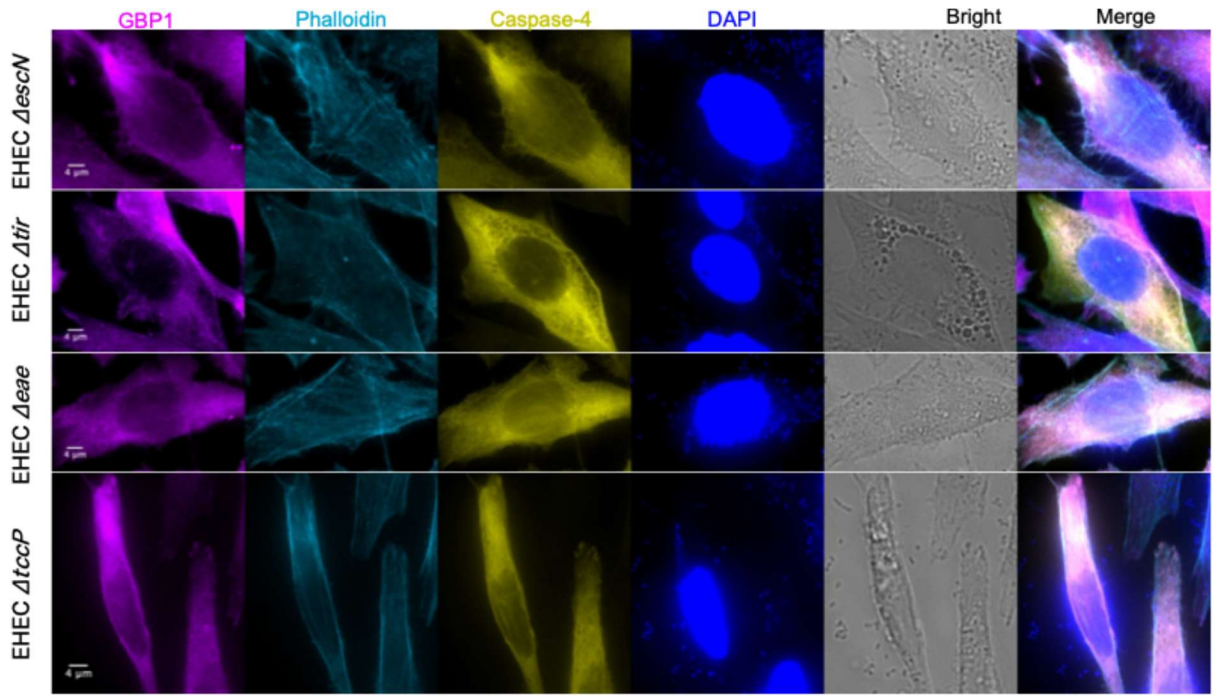

Figure 15: Pathogen-induced actin polymerisation is necessary for GBP1 and Caspase-4 recruitment.

Representative immunofluorescence image of HeLa WT YFP-Casp-4^{C258S} cells infected with (A) EPEC or (B) EHEC mutants for 3 hours. Image representative of n = 3 independent experiments. Cells were stained with GBP1-647 to visualise GBP1, Phalloidin-568 to visualise actin and Hoechst Dye to visualise nuclei. Scale bar = 4 µm.

A portion of the results described in this section have been published as a pre-print (Bennison et. al., 2025), which may lead to high similarity in parts.

Pyroptosis was tested in IFNγ-primed HeLa WT YFP-Casp-4^{C258S} cells infected with EHEC actin-pedestal or T3SS mutants. We observed significantly lower pyroptotic response upon infection measured at 8 hours post infection with the mutants as compared to EHEC WT (Fig. 16), suggesting that actin pedestal formation is necessary for pyroptotic response in IFNγ-primed HeLa cells.

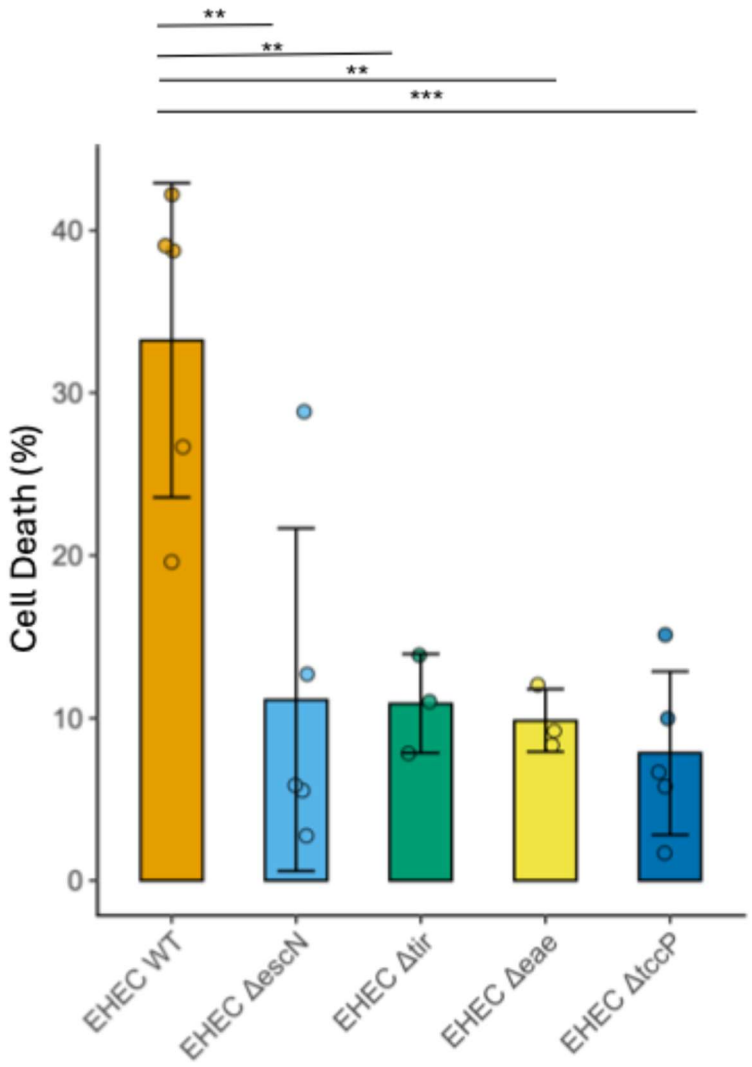

Figure 16: Pathogen-induced actin polymerisation is necessary for pyroptosis.

Percentage pyroptosis as measured by PI uptake assays of IFNγ-treated HeLa WT cells infected with EHEC WT or functional mutants. Measurements were plotted at 8 hours post infection. Mean ± SD from n = 3 independent experiments are depicted for EHEC *Δeae* and *Δtir* mutants, and n = 5 independent experiments for EHEC WT, *ΔescN* and *ΔtccP*.

A portion of the results described in this section have been published as a pre-print (Bennison et. al., 2025), which may lead to high similarity in parts.

Data Information: **P ≤ 0.01, ***P ≤ 0.001 for indicated comparisons in figure from one-way mixed model ANOVA.

3.8. Tir-induced actin polymerisation is sufficient for GBP1 and Caspase-4 recruitment

To further understand the molecular mechanism by which GBP1 and Caspase-4 detect extracellular pathogen infections, a pathogen-free system was designed. LPS is detected by GBP1 and Caspase-4 in the case of intracellular Gram-negative pathogens such as Salmonella. However, extracellular pathogens such as EPEC and EHEC do not enter the cell and thus it is unclear what role LPS may play, if any, and whether any other molecular signals are involved.

To decouple the effects of LPS and Tir-induced actin pedestal formation, we used a pathogen-free Tir-clustering system. HeLa cells expressing a chimeric receptor FcγRIIA-Tir were treated with beads coated with human immunoglobulin G (IgG) for 15 minutes. The chimeric receptor FcγRIIA-Tir consists of the C-terminal of Tir fused with the constant domain of human immunoglobulin receptor (FcγRIIA). In neutrophils, the Fcγ receptor initiates immunoreceptor tyrosine-based activation motif (ITAM) signalling upon cross-linking of receptors through immunoglobulin interaction (Isakov, 1997). Hence, when HeLa cells expressing FcγRIIA-Tir are treated with beads coated with IgG, the Fcγ portions of the receptors cross-link extracellularly, leading to Tir clustering intracellularly, and signal formation of actin pedestals (Fig. 17). BSA-coated beads were used as a negative control to ensure bead treatment did not cause actin polymerisation.

A portion of the results described in this section have been published as a pre-print (Bennison et. al., 2025), which may lead to high similarity in parts.

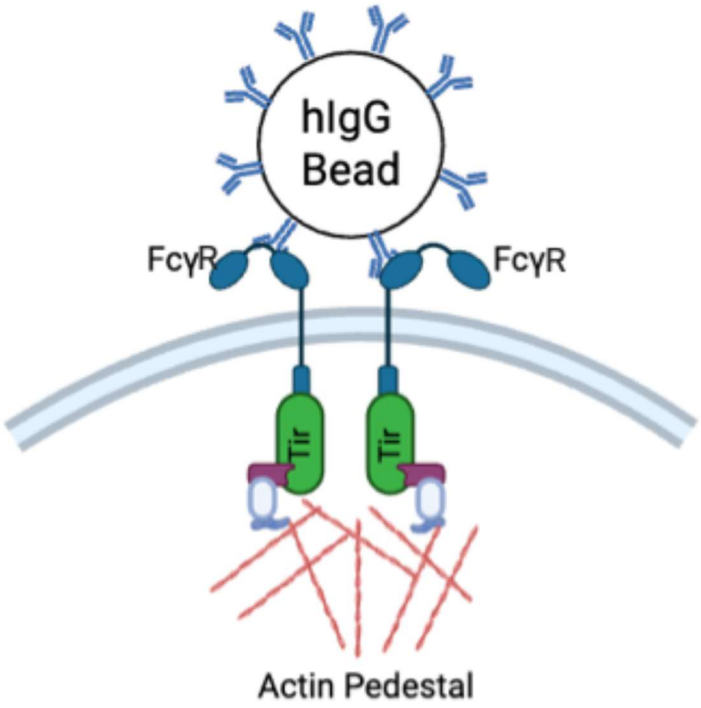

Figure 17: Schematic depicting pathogen-free bead-clustering assays. Created in BioRender.

Chimeric FcγRIIA-Tir receptors cluster upon interaction of the constant Fcγ domain of the receptor with polystyrene beads coated with human IgG, leading to intracellular Tir clustering and actin polymerisation.

We observed that only cells treated with IgG-coated beads formed actin pedestals and GBP1 and Caspase-4 trafficked to these pedestals (Fig. 18). Thus, we inferred that Tir-clustering and actin pedestal formation is a sufficient condition for GBP1 and Caspase-4 recruitment to these pedestals, and LPS, other bacterial effectors or ligands may not be required.

A portion of the results described in this section have been published as a pre-print (Bennison et. al., 2025), which may lead to high similarity in parts.

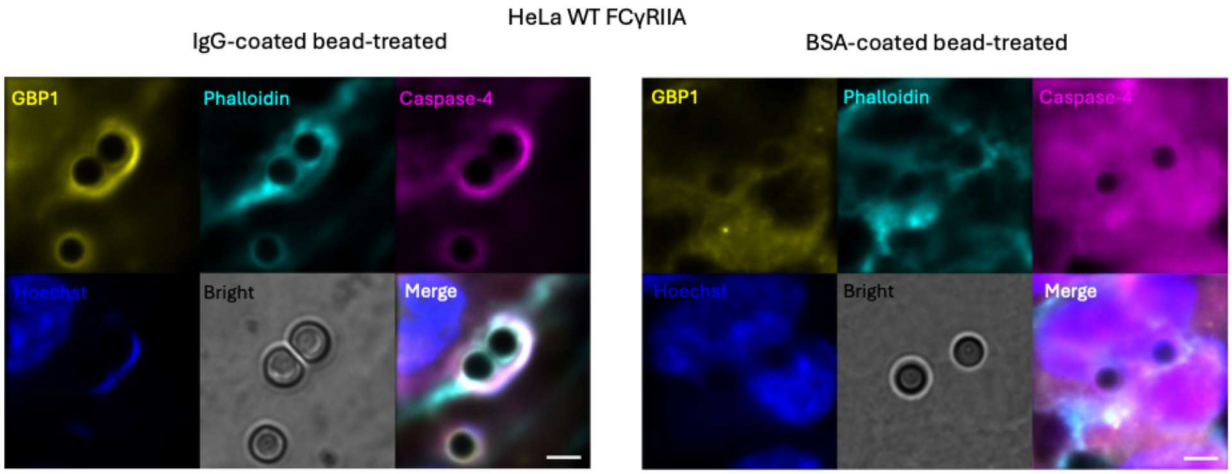

Figure 18: Tir-induced actin polymerisation is sufficient for GBP1 and Caspase-4 recruitment.

Representative immunofluorescence image of HeLa WT FcγRIIA-Tir cells treated with beads coated with human IgG or BSA for 15 minutes followed by incubation for 3 hours. Image representative of n = 3 independent experiments. Cells were stained with GBP1-647 to visualise GBP1, Phalloidin-568 to visualise actin and Hoechst Dye to visualise nuclei. Scale bar = 4 µm

3.9. Tir-induced actin polymerisation is not sufficient for pyroptosis

Upon observing GBP1 and Caspase-4 recruitment to sites of Tir clustering-induced actin polymerisation, we asked whether recruitment is sufficient to lead to pyroptotic cell death. HeLa cells expressing the chimeric receptor FcγRIIA-Tir were treated with beads coated with human immunoglobulin G (IgG) for 15 minutes, and pyroptosis was assessed for 24 hours. However, we observed no discernible cell death over this period (Fig. 19), suggesting that the recruitment and activation of GBP1 and Caspase-4 to actin-rich structures may be uncoupled processes.

A portion of the results described in this section have been published as a pre-print (Bennison et. al., 2025), which may lead to high similarity in parts.

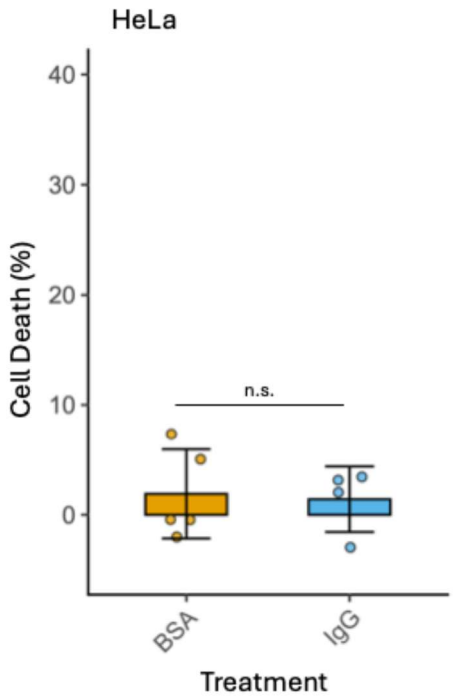

Figure 19: Tir-induced actin polymerisation is not sufficient for pyroptosis.

Percentage pyroptosis as measured by PI uptake assays of IFNγ-treated HeLa WT FcγRIIA-Tir cells treated with BSA or IgG beads for 15 minutes. Measurements were plotted at 8 hours post infection. Mean ± SD from n = 4 independent experiments are depicted for IgG bead treatment and n = 5 independent experiments for BSA bead treatment.

Data Information: P > 0.05 was evaluated for indicated one-way mixed model ANOVA.

A portion of the results described in this section have been published as a pre-print (Bennison et. al., 2025), which may lead to high similarity in parts.

4. Discussion

Here we have shown that GBP1 and caspase-4 are crucial innate immune proteins that detect and respond to infections of extracellular intestinal pathogens. A/E pathogen-induced pyroptosis in intestinal epithelial cells was caspase-4 and gasdermin-D-mediated, and it did not involve the NLRP3-caspase-1 inflammasome. GBP1 silencing in intestinal epithelial cells reduced pyroptotic cell death upon EPEC infection. GBP2 was weakly recruited to a small proportion of pedestals whereas GBP3,4 and 5 were not recruited to actin pedestals. We demonstrated that caspase-4 is recruited to pedestals at sites of EPEC infection in a GBP-1-dependent manner and that the recruitment of GBP1 and caspase-4 to pedestals is independent of LPS as they also traffic to sterile pedestals formed upon artificial Tir-clustering through a pathogen-free bead-clustering system.

Past work has shown that EPEC-induced pyroptosis in macrophages is NLRP3-caspase-1-dependent, since inhibiting NLRP3 with MCC950 reduced pyroptotic cell death (Goddard *et al.*, 2019). This is unusual since caspase-4-mediated LPS sensing in many cell lines directly lea`wds to pyroptosis instead of being NLRP3-caspase-1-dependent (Fisch *et al.*, 2019; Wu *et al.*, 2022). Hence, the lack of reduction in pyroptosis we observed upon MCC950 treatment suggests that caspase-4-mediated GSDMD cleavage is the major pyroptosis pathway in IFNγ-primed epithelial cells during EPEC infection.

During intracellular pathogen infection in epithelial cells, GBPs make an oligomeric coat on bacterial LPS, improving its accessibility to Caspase-4 to activate it and lead to pyroptosis (Wandel *et al.*, 2017; Fisch *et al.*, 2019). The reduced pyroptotic response upon GBP1 silencing in conjunction with the previous discovery that GBP1 is trafficked to EPEC-induced actin pedestals in HeLa cells (Bennison *et al.*, 2025), suggests that GBP1 plays an essential role in caspase-4 activity in pyroptosis in epithelial cells upon EPEC infection.

The lack of GBP3,4 and 5 recruitment and infrequent GBP2 recruitment suggests that the multi-GBP complex formed around intracellular Gram-negative bacteria may not be required for initiating pyroptotic cell death in our system, and a yet-unknown mechanism involving GBP1-based recognition and caspase-4 recruitment may be

sufficient. Inducible expression of GBP1 mutants in GBP1$^{-/-}$ HeLa cells may help further elucidate the mechanism of GBP1 sensing. Preliminary data from ongoing experiments by other members in the lab suggest that GBP1 mutants lacking GTPase activity or LPS-sensing functionality (but still binding GTP) traffic to actin pedestals but do not support pyroptosis, however, mutants lacking GTP-binding do not traffic to pedestals. This may indicate a signalling role for GTP-binding at actin pedestals to recruit GBP1 independent of LPS, however LPS-sensing may be required for further activation steps.

GBP1-dependent caspase-4 recruitment to EPEC-induced actin pedestals corroborates with previous findings on GBP1-dependent caspase-4 recruitment during intracellular Gram-negative infections in epithelial cells (Fisch *et al.*, 2019). GBP1 and caspase-4 recruitment to “sterile” Fcγ-Tir clustering induced-pedestals in this pathogen-free system shows that GBP1-dependent caspase-4 recruitment to actin pedestals is LPS-independent. A GBP1 interactor in the context of recruitment to pedestals may be actin itself (Ostler *et al.*, 2014), however, the interaction must be context-dependent, as GBP1 does not target *Shigella* and *Burkholderia* actin “comet-tails” in the cytoplasm. Instead, in these scenarios, high concentrations of cytosolic LPS are most likely a sufficient signal for GBP1 recruitment directly to bacterial membranes. Low concentrations of LPS upon EPEC and EHEC infection, farnesylation of GBP1, and membrane proximity of EPEC/EHEC actin pedestals may point to a plausible alternative mechanism of actin sensing by GBP1 near the cell membrane.

The lack of pyroptosis upon FcγR-Tir clustering could be explained by insufficient receptor expression or insufficient IgG coating leading to low amounts of clustering which may generate a signal below the required threshold to initiate caspase-4 activation. Inducible expression of the chimeric receptor or increased IgG concentration may help test these possibilities. Another more likely reason for the lack of pyroptosis in this system may be the requirement of a different molecule such as LPS for caspase-4 activation uncoupled from recruitment. Past work has shown that LPS can enter the cell during extracellular pathogen infection in the form of endocytosed outer vesicle membranes of EPEC/EHEC which contain LPS. LPS entry into the cell is dependent on Ca^{2+} influx through TRPV2 ion channels. GBP1 and caspase-4 are recruited to LPS-containing Gram-negative bacterial outer

membrane vesicles during intracellular infections and form complexes to detect LPS, activate caspase-4-mediated GSDMD cleavage and cleave pro-IL-18, leading to pyroptotic response (Zhong *et al.*, 2020, 2022). Based on these observations, it is possible that LPS sensing may play a role in Caspase activation, and GBP1 and caspase-4 may form LPS-sensing complexes near actin pedestals. Hence, we propose a 3-step mechanism for A/E-pathogen-induced pyroptosis:

1) Trafficking of GBP1 to actin pedestals

2) Recruitment of caspase-4 to pedestals in a GBP1-dependent manner

3) Activation of caspase-4 activity leading to pyroptosis

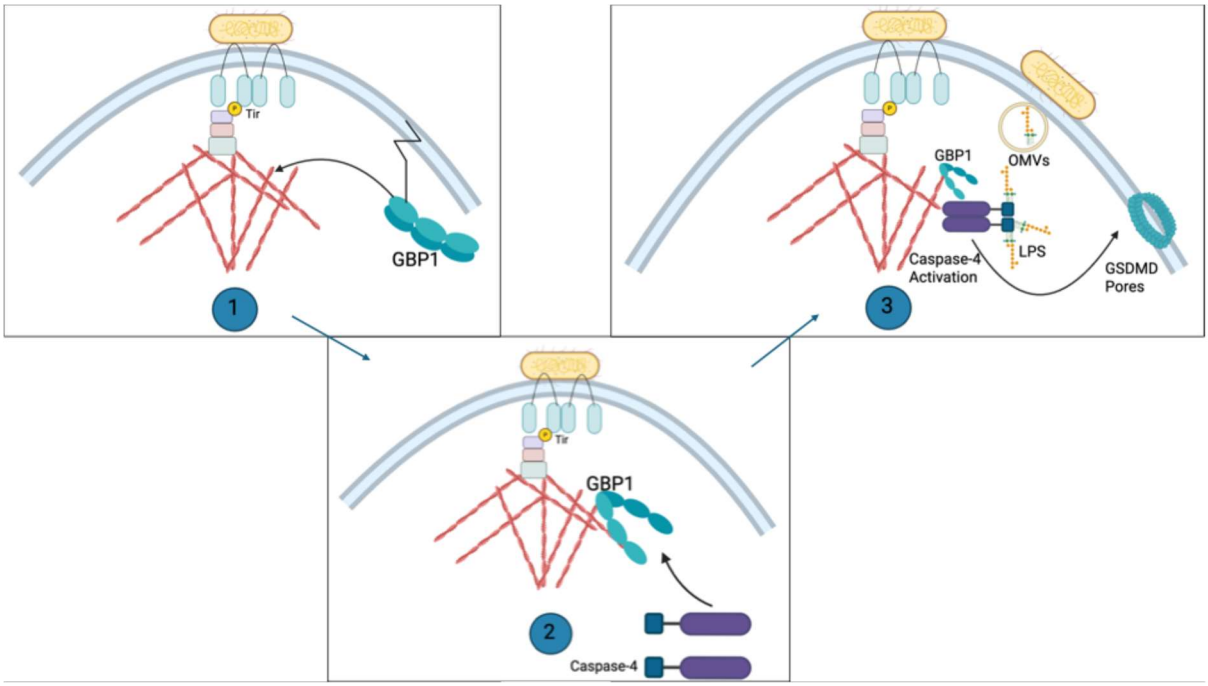

Figure 20: Proposed mechanism for GBP1 and caspase-4-induced pyroptosis in epithelial cells upon EPEC infection. Created in BioRender.

A 3-step mechanism is proposed:

1) Trafficking of GBP1 to actin pedestals

2) Recruitment of caspase-4 to pedestals in a GBP1-dependent manner

3) Activation of caspase-4 activity leading to pyroptosis.

LPS seems to be the most likely candidate for caspase-4 activation; however, other mechanisms may also exist. The relatively low concentration of intracellular LPS upon extracellular pathogen infection leaves room for the possibility that other

pathogenic effectors may activate these sensors. Although no EPEC or EHEC effectors are known to be effectively recognised by GBP1 and caspase-4, many tools exist to test for these interactions. There exist EPEC strains lacking all effectors (EPEC 0) or expressing only single or a few LEE and non-LEE effectors (Zhong *et al.*, 2020), and infection with these EPEC mutant strains may help shed some light on other possible molecular interactions between caspase-4 and pathogenic effectors. To decouple these effects from LPS, transfection of these proteins or inducible expression directly in cell lines alongside Fcγ-Tir bead-clustering assays may be another possibility to look for other interactors of caspase-4.

The role of GBP2 in response to extracellular infections remains unclear. We observed weak localisation of GBP2 in the vicinity of actin pedestals, and no effect of GBP2 silencing on pyroptosis, indicating that GBP2 may have a minor role in sensing actin pedestals. During intracellular *Salmonella* infections, GBP2 has been observed to be recruited to the bacterial surface in a GBP1-dependent manner (Fisch *et al.*, 2019). Thus, it will be interesting to observe GBP2 recruitment in GBP1$^{-/-}$ cells. Testing for pyroptosis in GBP1$^{-/-}$ cells silenced for GBP2 can also be an important step in identifying a potential GBP1-independent role of GBP2 in this process.

Limitations of the study and Future Directions

The majority of our experiments were conducted in HeLa which is a cervical cancer cell line and does not physiologically mimic the natural host of A/E pathogens. HT29 and CL40 cell lines are better for this purpose as they are primary-like intestinal epithelial cell lines. However, they still lack context of tissues and the extracellular matrix which play important roles in infection and detection mechanisms. Performing these experiments in organoids or organ-on-chip models will help further confirm these observations and test them in a more physiologically relevant context. *C. rodentium* infections in mouse models can model these infections *in vivo* and provide further clues towards dissecting immune mechanisms.

A limitation of our FcγR-Tir bead clustering system is that there is no control over the expression of the chimeric FcγR-Tir receptor in HeLa cells, and no control on the quantity of human IgG coating the polystyrene beads. Introducing inducible expression of the chimeric receptor and titrating bead coating may help improve

assay sensitivity. It may also improve cell viability as HeLa cells expressing this receptor grow slower and appear sicker.

Testing the role of GBP3,4 and 5 in pyroptosis through cell death assays may be another direction to further the prospects presented in this study. They may be recruited to pedestals at later time points and play auxiliary roles in immune responses to these infections.

To summarise, we uncovered a novel immune response of epithelial cells against extracellular A/E pathogen infections through LPS-independent sensing and recruitment of GBP1 by yet-unknown mechanisms. The discovery that intracellular LPS sensors can detect extracellular pathogens and initiate successful defensive responses against them may guide future approaches to investigate other intracellular sensors of pathogenic molecular patterns. It can further broaden our understanding of cell-autonomous immune mechanisms of non-immune cells acting as a first line of defence against potentially deadly pathogens.

5. References

Al-Qahtani, AA, Alhamlan, FS, and Al-Qahtani, AA (2024). Pro-Inflammatory and Anti-Inflammatory Interleukins in Infectious Diseases: A Comprehensive Review. Tropical Medicine and Infectious Disease 9, 13.

Bennison, DJ, Chaudhary, I, Chaudhuri, D, Wong, JCN, Biswas, P, Zhong, Q, Kallemeijn, WW, Guenot, M, Talman, AM, Frickel, E-M, *et al.* (2025). GBP1 recruitment to actin-rich pedestals induced by extracellular Gram negative bacteria promotes pyroptosis. bioRxiv, 2025.09.25.678451.

Berger, CN, Crepin, VF, Jepson, MA, Arbeloa, A, and Frankel, G (2009). The mechanisms used by enteropathogenic Escherichia coli to control filopodia dynamics. Cellular Microbiology 11, 309–322.

Britzen-Laurent, N, Bauer, M, Berton, V, Fischer, N, Syguda, A, Reipschläger, S, Naschberger, E, Herrmann, C, and Stürzl, M (2010). Intracellular Trafficking of Guanylate-Binding Proteins Is Regulated by Heterodimerization in a Hierarchical Manner. PLOS ONE 5, e14246.

Broz, P, and Dixit, VM (2016). Inflammasomes: mechanism of assembly, regulation and signalling. Nat Rev Immunol 16, 407–420.

Broz, P, Newton, K, Lamkanfi, M, Mariathasan, S, Dixit, VM, and Monack, DM (2010). Redundant roles for inflammasome receptors NLRP3 and NLRC4 in host defense against Salmonella. J Exp Med 207, 1745–1755.

Cabrera-Sosa, L, and Ochoa, TJ (2020). Escherichia coli Diarrhea. Hunter’s Tropical Medicine and Emerging Infectious Diseases.

Ceballos-Olvera, I, Sahoo, M, Miller, MA, Barrio, L del, and Re, F (2011). Inflammasome-dependent Pyroptosis and IL-18 Protect against Burkholderia pseudomallei Lung Infection while IL-1β Is Deleterious. PLOS Pathogens 7, e1002452.

Chaudhuri, D, Mukherjee, D, Shenoy, AR, and Visweswariah, SS (2026). Infectious Diarrhea in Early Childhood across the Global South: Etiologic Diversity and Pathogenic Mechanisms. ACS Infect Dis 12, 471–489.

Collins, JW, Keeney, KM, Crepin, VF, Rathinam, VAK, Fitzgerald, KA, Finlay, BB, and Frankel, G (2014). Citrobacter rodentium: infection, inflammation and the microbiota. Nat Rev Microbiol 12, 612–623.

Crepin, VF, Girard, F, Schüller, S, Phillips, AD, Mousnier, A, and Frankel, G (2010). Dissecting the role of the Tir:Nck and Tir:IRTKS/IRSp53 signalling pathways in vivo. Molecular Microbiology 75, 308–323.

Dean, P, and Kenny, B (2009). The effector repertoire of enteropathogenic E. coli: ganging up on the host cell. Current Opinion in Microbiology 12, 101–109.

Deng, W, Vallance, BA, Li, Y, Puente, JL, and Finlay, BB (2003). Citrobacter rodentium translocated intimin receptor (Tir) is an essential virulence factor needed for actin condensation, intestinal colonization and colonic hyperplasia in mice. Molecular Microbiology 48, 95–115.

Donnenberg, MS, Girón, JA, Nataro, JP, and Kaper, JB (1992). A plasmid-encoded type IV fimbrial gene of enteropathogenic Escherichia coli associated with localized adherence. Molecular Microbiology 6, 3427–3437.

Eldridge, MJG, Sanchez-Garrido, J, Hoben, GF, Goddard, PJ, and Shenoy, AR (2017). The Atypical Ubiquitin E2 Conjugase UBE2L3 Is an Indirect Caspase-1 Target and Controls IL-1β Secretion by Inflammasomes. Cell Reports 18, 1285–1297.

Elliott, SJ, Wainwright, LA, McDaniel, TK, Jarvis, KG, Deng, Y, Lai, L-C, McNamara, BP, Donnenberg, MS, and Kaper, JB (1998). The complete sequence of the locus of enterocyte effacement (LEE) from enteropathogenic Escherichia coli E2348/69. Mol Microbiol 28, 1–4.

Fensterheim, BA, Young, JD, Luan, L, Kleinbard, RR, Stothers, CL, Patil, NK, McAtee-Pereira, AG, Guo, Y, Trenary, I, Hernandez, A, *et al.* (2018). The TLR4 Agonist Monophosphoryl Lipid A Drives Broad Resistance to Infection via Dynamic Reprogramming of Macrophage Metabolism. J Immunol 200, 3777–3789.

Fisch, D, Bando, H, Clough, B, Hornung, V, Yamamoto, M, Shenoy, AR, and Frickel, E (2019). Human GBP1 is a microbe-specific gatekeeper of macrophage apoptosis and pyroptosis. EMBO J 38, EMBJ2018100926.

Frankel, G, and Phillips, AD (2008). Attaching effacing Escherichia coli and paradigms of Tir-triggered actin polymerization: getting off the pedestal. Cellular Microbiology 10, 549–556.

Frankel, G, Phillips, AD, Rosenshine, I, Dougan, G, Kaper, JB, and Knutton, S (1998). Enteropathogenic and enterohaemorrhagic Escherichia coli : more subversive elements. Molecular Microbiology 30, 911–921.

Ghosh, A, Praefcke, GJK, Renault, L, Wittinghofer, A, and Herrmann, C (2006). How guanylate-binding proteins achieve assembly-stimulated processive cleavage of GTP to GMP. Nature 440, 101–104.

Goddard, PJ, Sanchez-Garrido, J, Slater, SL, Kalyan, M, Ruano-Gallego, D, Marchès, O, Fernández, LÁ, Frankel, G, and Shenoy, AR (2019). Enteropathogenic Escherichia coli Stimulates Effector-Driven Rapid Caspase-4 Activation in Human Macrophages. Cell Reports 27, 1008-1017.e6.

Gruenheid, S, DeVinney, R, Bladt, F, Goosney, D, Gelkop, S, Gish, GD, Pawson, T, and Finlay, BB (2001). Enteropathogenic E. coli Tir binds Nck to initiate actin pedestal formation in host cells. Nat Cell Biol 3, 856–859.

Gruenheid, S, Sekirov, I, Thomas, NA, Deng, W, O'Donnell, P, Goode, D, Li, Y, Frey, EA, Brown, NF, Metalnikov, P, *et al.* (2004). Identification and characterization of

NleA, a non-LEE-encoded type III translocated virulence factor of enterohaemorrhagic Escherichia coli O157:H7. Molecular Microbiology 51, 1233–1249.

Ihim, SA, Abubakar, SD, Zian, Z, Sasaki, T, Saffarioun, M, Maleknia, S, and Azizi, G (2022). Interleukin-18 cytokine in immunity, inflammation, and autoimmunity: Biological role in induction, regulation, and treatment. Front Immunol 13.

Isakov, N (1997). Immunoreceptor tyrosine-based activation motif (ITAM), a unique module linking antigen and Fc receptors to their signaling cascades. Journal of Leukocyte Biology 61, 6–16.

Janeway, CA (1989). Approaching the asymptote? Evolution and revolution in immunology. Cold Spring Harb Symp Quant Biol 54 Pt 1, 1–13.

Jeong, J-Y, Yim, H-S, Ryu, J-Y, Lee, HS, Lee, J-H, Seen, D-S, and Kang, SG (2012). One-Step Sequence- and Ligation-Independent Cloning as a Rapid and Versatile Cloning Method for Functional Genomics Studies. Applied and Environmental Microbiology 78, 5440–5443.

Kelly, M, Hart, E, Mundy, R, Marchès, O, Wiles, S, Badea, L, Luck, S, Tauschek, M, Frankel, G, Robins-Browne, RM, *et al.* (2006). Essential Role of the Type III Secretion System Effector NleB in Colonization of Mice by Citrobacter rodentium. Infection and Immunity 74, 2328–2337.

Kenny, B, DeVinney, R, Stein, M, Reinscheid, DJ, Frey, EA, and Finlay, BB (1997). Enteropathogenic E. coli (EPEC) Transfers Its Receptor for Intimate Adherence into Mammalian Cells. Cell 91, 511–520.

Kenny, B, and Finlay, BB (1997). Intimin-dependent binding of enteropathogenic Escherichia coli to host cells triggers novel signaling events, including tyrosine phosphorylation of phospholipase C-gamma1. Infection and Immunity 65, 2528–2536.

Kim, B-H, Shenoy, AR, Kumar, P, Das, R, Tiwari, S, and MacMicking, JD (2011). A Family of IFN-γ–Inducible 65-kD GTPases Protects Against Bacterial Infection. Science 332, 717–721.

Kirshner, H, Aguet, F, Sage, D, and Unser, M (2013). 3-D PSF fitting for fluorescence microscopy: implementation and localization application. Journal of Microscopy 249, 13–25.

Knutton, S, Lloyd, DR, and McNeish, AS (1987). Adhesion of enteropathogenic Escherichia coli to human intestinal enterocytes and cultured human intestinal mucosa. Infection and Immunity 55, 69–77.

Kotloff, KL, Nataro, JP, Blackwelder, WC, Nasrin, D, Farag, TH, Panchalingam, S, Wu, Y, Sow, SO, Sur, D, Breiman, RF, *et al.* (2013). Burden and aetiology of diarrhoeal disease in infants and young children in developing countries (the Global Enteric Multicenter Study, GEMS): a prospective, case-control study. The Lancet 382, 209–222.

Kuhm, T, Taisne, C, de Agrela Pinto, C, Gross, L, Giannopoulou, EA, Huber, ST, Pardon, E, Steyaert, J, Tans, SJ, and Jakobi, AJ (2025). Structural basis of antimicrobial membrane coat assembly by human GBP1. Nat Struct Mol Biol 32, 172–184.

Launders, N, Byrne, L, Jenkins, C, Harker, K, Charlett, A, and Adak, GK (2016). Disease severity of Shiga toxin-producing *E. coli* O157 and factors influencing the development of typical haemolytic uraemic syndrome: a retrospective cohort study, 2009–2012. BMJ Open 6, e009933.

Levine, MyronM, Nalin, DavidR, Hornick, RichardB, Bergquist, ErickJ, Waterman, DanielH, Young, CharlesR, Sotman, S, and Rowe, B (1978). ESCHERICHIA COLI STRAINS THAT CAUSE DIARRHŒA BUT DO NOT PRODUCE HEAT-LABILE OR HEAT-STABLE ENTEROTOXINS AND ARE NON-INVASIVE. The Lancet 311, 1119–1122.

Li, L-H, Chen, T-L, Chiu, H-W, Hsu, C-H, Wang, C-C, Tai, T-T, Ju, T-C, Chen, F-H, Chernikov, OV, Tsai, W-C, *et al.* (2020). Critical Role for the NLRP3 Inflammasome in Mediating IL-1β Production in Shigella sonnei-Infected Macrophages. Front Immunol 11.

Li, Y, Lin, X, Wang, W, Wang, W, Cheng, S, Huang, Y, Zou, Y, Ke, J, and Zhu, L (2022). The Proinflammatory Role of Guanylate-Binding Protein 5 in Inflammatory Bowel Diseases. Front Microbiol 13.

Luchetti, G, Miner, MV, Peterson, RM, Scott, WP, Krishnamoorthy, P, Kofoed, EM, Jimenez, AG, Zhang, H, Tan, MW, Reja, R, *et al.* (2025). Enteropathogenic bacteria evade ROCK-driven epithelial cell extrusion. Nature 648, 166–172.

Ma, C, Wickham, ME, Guttman, JA, Deng, W, Walker, J, Madsen, KL, Jacobson, K, Vogl, WA, Finlay, BB, and Vallance, BA (2006). Citrobacter rodentium infection causes both mitochondrial dysfunction and intestinal epithelial barrier disruption in vivo: role of mitochondrial associated protein (Map). Cellular Microbiology 8, 1669–1686.

Majowicz, SE, Scallan, E, Jones-Bitton, A, Sargeant, JM, Stapleton, J, Angulo, FJ, Yeung, DH, and Kirk, MD (2014). Global Incidence of Human Shiga Toxin–Producing Escherichia coli Infections and Deaths: A Systematic Review and Knowledge Synthesis. Foodborne Pathogens and Disease 11, 447–455.

Man, SM, Hopkins, LJ, Nugent, E, Cox, S, Glück, IM, Tourlomousis, P, Wright, JA, Cicuta, P, Monie, TP, and Bryant, CE (2014). Inflammasome activation causes dual recruitment of NLRC4 and NLRP3 to the same macromolecular complex. Proceedings of the National Academy of Sciences 111, 7403–7408.

Marchès, O, Covarelli, V, Dahan, S, Cougoule, C, Bhatta, P, Frankel, G, and Caron, E (2008). EspJ of enteropathogenic and enterohaemorrhagic Escherichia coli inhibits opsono-phagocytosis. Cellular Microbiology 10, 1104–1115.

McDaniel, TK, Jarvis, KG, Donnenberg, MS, and Kaper, JB (1995). A genetic locus of enterocyte effacement conserved among diverse enterobacterial pathogens. Proceedings of the National Academy of Sciences 92, 1664–1668.

Mishra, V, Crespo-Puig, A, McCarthy, C, Masonou, T, Glegola-Madejska, I, Dejoux, A, Dow, G, Eldridge, MJG, Marinelli, LH, Meng, M, *et al.* (2023). IL-1β turnover by the UBE2L3 ubiquitin conjugating enzyme and HECT E3 ligases limits inflammation. Nat Commun 14, 4385.

Mullineaux-Sanders, C, Sanchez-Garrido, J, Hopkins, EGD, Shenoy, AR, Barry, R, and Frankel, G (2019). Citrobacter rodentium–host–microbiota interactions: immunity, bioenergetics and metabolism. Nat Rev Microbiol 17, 701–715.

Murphey, ED, Fang, G, Varma, TK, and Sherwood, ER (2007). IMPROVED BACTERIAL CLEARANCE AND DECREASED MORTALITY CAN BE INDUCED BY LPS TOLERANCE AND IS NOT DEPENDENT UPON IFN-γ. Shock 27, 289.

Murphey, ED, and Sherwood, ER (2008). Pretreatment with the Gram-positive bacterial cell wall molecule peptidoglycan improves bacterial clearance and decreases inflammation and mortality in mice challenged with *Pseudomonas aeruginosa*. Microbes and Infection 10, 1244–1250.

Nantais, DE, Schwemmle, M, Stickney, JT, Vestal, DJ, and Buss, JE (1996). Prenylation of an interferon-γ-induced GTP-binding protein: the human guanylate binding protein, huGBP1. Journal of Leukocyte Biology 60, 423–431.

Ng, CT, Fong, LY, and Abdullah, MNH (2023). Interferon-gamma (IFN-γ): Reviewing its mechanisms and signaling pathways on the regulation of endothelial barrier function. Cytokine 166, 156208.

Ostler, N, Britzen-Laurent, N, Liebl, A, Naschberger, E, Lochnit, G, Ostler, M, Forster, F, Kunzelmann, P, Ince, S, Supper, V, *et al.* (2014). Gamma Interferon-Induced Guanylate Binding Protein 1 Is a Novel Actin Cytoskeleton Remodeling Factor. Molecular and Cellular Biology 34, 196–209.

Pallett, MA, Crepin, VF, Serafini, N, Habibzay, M, Kotik, O, Sanchez-Garrido, J, Di Santo, JP, Shenoy, AR, Berger, CN, and Frankel, G (2017). Bacterial virulence factor inhibits caspase-4/11 activation in intestinal epithelial cells. Mucosal Immunology 10, 602–612.

Pearson, JS, Giogha, C, Lung, TWF, and Hartland, EL (2016). The Genetics of Enteropathogenic Escherichia coli Virulence. Annual Review of Genetics 50, 493–513.

Petty, NK, Bulgin, R, Crepin, VF, Cerdeño-Tárraga, AM, Schroeder, GN, Quail, MA, Lennard, N, Corton, C, Barron, A, Clark, L, *et al.* (2010). The Citrobacter rodentium Genome Sequence Reveals Convergent Evolution with Human Pathogenic Escherichia coli. Journal of Bacteriology 192, 525–538.

Phillips, N, Hayward, RD, and Koronakis, V (2004). Phosphorylation of the enteropathogenic E. coli receptor by the Src-family kinase c-Fyn triggers actin pedestal formation. Nat Cell Biol 6, 618–625.

Rivera-Cuevas, Y, Clough, B, and Frickel, E-M (2023). Human guanylate-binding proteins in intracellular pathogen detection, destruction, and host cell death induction. Current Opinion in Immunology 84, 102373.

Romero, CD, Varma, TK, Hobbs, JB, Reyes, A, Driver, B, and Sherwood, ER (2011). The Toll-Like Receptor 4 Agonist Monophosphoryl Lipid A Augments Innate Host Resistance to Systemic Bacterial Infection. Infection and Immunity 79, 3576–3587.

Sage, D, Donati, L, Soulez, F, Fortun, D, Schmit, G, Seitz, A, Guiet, R, Vonesch, C, and Unser, M (2017). DeconvolutionLab2: An open-source software for deconvolution microscopy. Methods 115, 28–41.

Sanchez-Garrido, J, Slater, SL, Clements, A, Shenoy, AR, and Frankel, G (2020). Vying for the control of inflammasomes: The cytosolic frontier of enteric bacterial pathogen–host interactions. Cellular Microbiology 22, e13184.

Santos, JC, Boucher, D, Schneider, LK, Demarco, B, Dilucca, M, Shkarina, K, Heilig, R, Chen, KW, Lim, RYH, and Broz, P (2020). Human GBP1 binds LPS to initiate assembly of a caspase-4 activating platform on cytosolic bacteria. Nat Commun 11, 3276.

Schauer, DB, and Falkow, S (1993). The eae gene of Citrobacter freundii biotype 4280 is necessary for colonization in transmissible murine colonic hyperplasia. Infection and Immunity 61, 4654–4661.

Schwemmle, M, and Staeheli, P (1994). The interferon-induced 67-kDa guanylate-binding protein (hGBP1) is a GTPase that converts GTP to GMP. Journal of Biological Chemistry 269, 11299–11305.

Shenoy, AR, Furniss, RCD, Goddard, PJ, and Clements, A (2018). Modulation of Host Cell Processes by T3SS Effectors. In: Escherichia Coli, a Versatile Pathogen, ed. G Frankel, and EZ Ron, Cham: Springer International Publishing, 73–115.

Shenoy, AR, Wellington, DA, Kumar, P, Kassa, H, Booth, CJ, Cresswell, P, and MacMicking, JD (2012). GBP5 Promotes NLRP3 Inflammasome Assembly and Immunity in Mammals. Science 336, 481–485.

Smith, JL, Fratamico, PM, and Gunther, NW (2014). Chapter Three - Shiga Toxin-Producing Escherichia coli. In: Advances in Applied Microbiology, ed. S Sariaslani, and GM Gadd, Academic Press, 145–197.

Smith, PD, Ochsenbauer-Jambor, C, and Smythies, LE (2005). Intestinal macrophages: unique effector cells of the innate immune system. Immunological Reviews 206, 149–159.

Sperandio, V, and Nguyen, Y (2012). Enterohemorrhagic E. coli (EHEC) pathogenesis. Frontiers in Cellular and Infection Microbiology Volume 2-2012.

Sperandio, V, and Pacheco, AR (2012). Shiga toxin in enterohemorrhagic E.coli: regulation and novel anti-virulence strategies. Frontiers in Cellular and Infection Microbiology Volume 2-2012.

Stuart, LM, Paquette, N, and Boyer, L (2013). Effector-triggered versus pattern-triggered immunity: how animals sense pathogens. Nat Rev Immunol 13, 199–206.

Tretina, K, Park, E-S, Maminska, A, and MacMicking, JD (2019). Interferon-induced guanylate-binding proteins: Guardians of host defense in health and disease. J Exp Med 216, 482–500.

Varma, TK, Durham, M, Murphey, ED, Cui, W, Huang, Z, Lin, CY, Toliver-Kinsky, T, and Sherwood, ER (2005). Endotoxin Priming Improves Clearance of Pseudomonas aeruginosa in Wild-Type and Interleukin-10 Knockout Mice. Infection and Immunity 73, 7340–7347.

Veerdonk, FL van de, Netea, MG, Dinarello, CA, and Joosten, LAB (2011). Inflammasome activation and IL-1β and IL-18 processing during infection. Trends in Immunology 32, 110–116.

Vingadassalom, D, Kazlauskas, A, Skehan, B, Cheng, H-C, Magoun, L, Robbins, D, Rosen, MK, Saksela, K, and Leong, JM (2009). Insulin receptor tyrosine kinase substrate links the E. coli O157:H7 actin assembly effectors Tir and EspFU during pedestal formation. Proceedings of the National Academy of Sciences 106, 6754–6759.

Wandel, MP, Kim, B-H, Park, E-S, Boyle, KB, Nayak, K, Lagrange, B, Herod, A, Henry, T, Zilbauer, M, Rohde, J, *et al.* (2020). Guanylate-binding proteins convert cytosolic bacteria into caspase-4 signaling platforms. Nat Immunol 21, 880–891.

Wandel, MP, Pathe, C, Werner, EI, Ellison, CJ, Boyle, KB, Malsburg, A von der, Rohde, J, and Randow, F (2017). GBPs Inhibit Motility of Shigella flexneri but Are Targeted for Degradation by the Bacterial Ubiquitin Ligase IpaH9.8. Cell Host & Microbe 22, 507-518.e5.

Weismehl, M, Chu, X, Kutsch, M, Lauterjung, P, Herrmann, C, Kudryashev, M, and Daumke, O (2024). Structural insights into the activation mechanism of antimicrobial GBP1. EMBO J 43, 615–636.

Weiss, SM, Ladwein, M, Schmidt, D, Ehinger, J, Lommel, S, Städing, K, Beutling, U, Disanza, A, Frank, R, Jänsch, L, *et al.* (2009). IRSp53 Links the Enterohemorrhagic E. coli Effectors Tir and EspFU for Actin Pedestal Formation. Cell Host & Microbe 5, 244–258.

Wilson, RK, Shaw, RK, Daniell, S, Knutton, S, and Frankel, G (2001). Role of EscF, a putative needle complex protein, in the type III protein translocation system of enteropathogenic Escherichia coli. Cellular Microbiology 3, 753–762.

Wong, ARC, Pearson, JS, Bright, MD, Munera, D, Robinson, KS, Lee, SF, Frankel, G, and Hartland, EL (2011). Enteropathogenic and enterohaemorrhagic Escherichia coli: even more subversive elements. Molecular Microbiology 80, 1420–1438.

Wu, Y, Pan, B, Zhang, Z, Li, X, Leng, Y, Ji, Y, Sun, K, and Chen, AF (2022). Caspase-4/11–Mediated Pulmonary Artery Endothelial Cell Pyroptosis Contributes to Pulmonary Arterial Hypertension. Hypertension 79, 536–548.

Xavier, A, Al-Zeer, MA, Meyer, TF, and Daumke, O (2020). hGBP1 Coordinates Chlamydia Restriction and Inflammasome Activation through Sequential GTP Hydrolysis. Cell Reports 31.

Zhong, Q, Chatterjee, S, Choudhary, JS, and Frankel, G (2022). EPEC-induced activation of the Ca2+ transporter TRPV2 leads to pyroptotic cell death. Molecular Microbiology 117, 480–492.

Zhong, Q, Roumeliotis, TI, Kozik, Z, Cepeda-Molero, M, Fernández, LÁ, Shenoy, AR, Bakal, C, Frankel, G, and Choudhary, JS (2020). Clustering of Tir during enteropathogenic E. coli infection triggers calcium influx–dependent pyroptosis in intestinal epithelial cells. PLOS Biology 18, e3000986.

Zong Minko, O, Mabika Mabika, R, Moyen, R, Mounioko, F, Ondjiangui, LF, and Yala, JF (2024). The Impact of Campylobacter, Salmonella, and Shigella in Diarrheal Infections in Central Africa (1998–2022): A Systematic Review. International Journal of Environmental Research and Public Health 21, 1635.

Diarrhoea. UNICEF DATA. Available at: https://data.unicef.org/topic/child-health/diarrhoeal-disease/. Accessed March 13, 2026.

Diarrhoeal disease. Available at: https://www.who.int/news-room/fact-sheets/detail/diarrhoeal-disease. Accessed March 13, 2026.

Trinh, T., et al., STBL2: An Escherichia coli strain... - Google Scholar. Available at: https://scholar.google.com/scholar?hl=en&as_sdt=0%2C5&q=Trinh%2C+T.%2C+et+al.%2C+STBL2%3A+An+Escherichia+coli+strain+for+the+stable+propagation+of+retroviral+clones+and+direct+repeat+sequences.+1994.+3%3A+p.+78-80.&btnG=. Accessed March 14, 2026.